博士論文

Novel protein MEIKIN regulates meiosis I specific kinetochore function in mouse

(新規タンパク質 MEIKIN はマウスの減数第一分裂特異的な動原体の機能を制御する)

平成 21 年度入学

東京大学大学院　農学生命科学研究科 応用生命工学専攻

氏　　名　　金　智慧

指導教員名　　渡邊　嘉典

Table of Contents

論文の内容の要旨

応用生命工学専攻
平成 21 年度博士課程　入学
氏　　名　　金　智慧
指導教員名　　渡邊　嘉典

論文題目

Novel protein MEIKIN regulates meiosis I specific kinetochore function in mouse

(新規タンパク質 MEIKIN はマウスの減数第一分裂特異的な動原体の機能を制御する.)

1. Introduction

In mitosis, one round of DNA replication and chromosome segregation generates two daughter cells. During meiosis, however, one round of DNA replication followed by two sequential rounds of chromosome segregation, meiosis I and II, generate haploid cells (eggs or sperm). Therefore, the chromosome dynamics in meiosis differ in many ways from those of mitosis.

The kinetochore, a multi-protein structure that links chromosomes to the spindle microtubules, regulates chromosome segregation in mitosis and meiosis. Thus, the kinetochore is an essential apparatus for proper chromosome segregation. In mitosis, sister kinetochores, the pair of kinetochores on each sister chromatid, are captured by microtubules originating from both spindle poles (bi-orientation), and segregate to opposite poles to generate two identical daughter cells (equational division).

In meiosis I, unlike in mitosis, homologous chromosomes are physically connected by chiasmata, thus forming a bivalent. In addition, sister kinetochores are captured by microtubules originating from the same pole (mono-orientation) in metaphase I, and centromeric cohesion is protected during anaphase I (cohesion protection). Consequently, homologous chromosomes separate to opposite poles while sister chromatids move to the same pole during meiosis I

(reductional division). Accordingly, the residual cohesion at the centromeres facilitates the equational segregation of sister chromatids in meiosis II.

The important meiotic functions of kinetochores, mono-orientation and cohesion protection, are widely conserved in eukaryotic organisms. So far, meiosis-specific kinetochore proteins that regulate mono-orientation and cohesion protection are only reported in yeasts (Moa1 in fission yeast; Spo13 and Mam1 in budding yeast). However, their homologs have remained unidentified in other organisms including humans.

2. MEIKIN, a meiosis I specific novel kinetochore protein in mouse

Fission yeast Moa1 binds directly to Cnp3 (CENP-C, a conserved core component of centromeric chromatin) and localizes to kinetochores where it acts for mono-orientation and cohesion protection. In order to identify such meiosis specific kinetochore factors in mouse, Dr. Nambu in our lab performed yeast two hybrid screening to search for mouse CENP-C binding proteins from a mouse testis cDNA library.

In that screening, our laboratory identified a novel meiosis-specific kinetochore protein, MEIKIN (Meiosis-specific kinetochore protein). RT-PCR examination revealed that MEIKIN expression is germ cell-specific (in male testes and female ovaries) and not detected in other organs. Also, immunostaining of germ cells (male spermatocytes and female oocytes) confirmed that MEIKIN localizes to kinetochores from meiotic prophase I to metaphase I, but never appears in meiosis II or mitosis. We showed that conserved C-terminus sequences in MEIKIN play an essential role in its localization at kinetochores, and that MEIKIN is largely conserved among vertebrates including humans. Therefore, we conclude that MEIKIN is a novel meiosis-I-specific kinetochore protein in mammals.

3. MEIKIN regulates cohesion protection and mono-orientation

To elucidate the function of MEIKIN, Dr. Ishiguro in our lab and Dr. Takeda in Kumamoto Univ. generated MEIKIN knockout (KO) mice. MEIKIN KO male and female mice are both infertile although their development is normal. Although no histological abnormalities were

observed in *Meikin*$^{-/-}$ testes and ovaries, an approximately 2-fold increase in the kinetochore number was observed in *Meikin*$^{-/-}$ round spermatids (post meiosis cells), which is indicative of meiotic cell division failure.

Intriguingly, *Meikin*$^{-/-}$ oocytes show premature separation of sister chromatids at the onset of anaphase I, and chromosome alignment defects in metaphase II. Indeed, REC8, a protein mediating sister chromatid cohesion in meiosis, is lost in metaphase II chromosomes in *Meikin*$^{-/-}$ oocytes, suggesting that MEIKIN regulates REC8 protection during anaphase I. To explore this defect, we tested Shugoshin-2 (SGO2, centromeric cohesion protector in meiosis I) localization in *Meikin*$^{-/-}$ and found that SGO2 localization is indeed decreased in *Meikin*$^{-/-}$ oocytes. Taken together, these observations indicate that MEIKIN regulates REC8 protection during meiosis I, and partially stabilizes SGO2 localization in oocytes. Similar results were obtained in *Meikin*$^{-/-}$ spermatocytes.

To analyze the potential function of MEIKIN in mono-orientation, we measured the distance between sister kinetochore pairs in *Meikin*$^{-/-}$ oocytes, and observed an approximately 20% increase in prometaphase I. Next, we examined chromosome alignment by deleting MEIKIN in an *Mlh1*$^{-/-}$ background. Because homologous chromosomes are not linked by chiasmata in *Mlh1*$^{-/-}$, meiosis I cells accumulate univalents that fail to align on the metaphase I plate. Presumably, the property of tightly fused sister kinetochores prevents bi-orientation of univalents. Strikingly, in *Mlh1*$^{-/-}$ *Meikin*$^{-/-}$ oocytes, univalents are aligned and bi-oriented along the metaphase I spindle equator. Similar results were observed in *Meikin*$^{-/-}$ spermatocytes.

Therefore, we conclude that MEIKIN plays an important role in promoting mono-orientation in addition to protecting centromeric cohesion during mouse meiosis I.

4. MEIKIN associated PLK1 regulates meiosis I specific kinetochore function

To address the molecular function of MEIKIN, our laboratory (Dr. Nambu) performed yeast two hybrid screening of MEIKIN as bait from a mouse testis cDNA library. We identified Polo-like kinase PLK1 as a MEIKIN binding protein, and our laboratory (Dr. Ishiguro) confirmed this by immunoprecipitation-MASS spectrometry. We confirmed that PLK1 is indeed

enriched to kinetochores, and, remarkably, that the PLK1 enrichment is largely impaired in *Meikin*$^{-/-}$ spermatocytes. However, in meiosis I oocytes, there is an approximately 40% reduction in PLK1 localization to kinetochores. These experiments reveal that PLK1 accumulation is in part dependent on MEIKIN during meiosis I.

To understand the function of PLK1 in kinetochore regulation, we inhibited PLK1 activity in meiosis I oocytes by adding BI 2536, a potent and selective inhibitor of PLK1. Surprisingly, transient BI 2536-treated wild type oocytes showed chromosome misalignment in metaphase II, implying that premature separation of sister chromatids occurs in anaphase I. Also, univalent alignment increased in BI 2536-treated *Mlh1−/−* oocytes as compared to non-treated *Mlh1−/−* oocytes. These experiments reveal that PLK1 activity is required for cohesion protection and the mono-orientation of sister kinetochores during meiosis I. We, therefore, conclude that MEIKIN regulates two important functions of meiotic kinetochores, cohesion protection and mono-orientation.

5. Conclusion

Here we identified a meiosis specific kinetochore protein, MEIKIN, in mouse that plays crucial roles in meiosis I. MEIKIN regulates two important functions of meiotic kinetochores, mono-orientation and cohesion protection, in part by stabilizing the localization of the centromeric cohesion protector Shugoshin-2. These functions are facilitated by the activity of Polo-like kinase PLK1, which is enriched to kinetochores dependent on MEIKIN.

MEIKIN is conserved in vertebrates including humans. Our group further revealed that MEIKIN is a functional homolog of fission yeast Moa1 and budding yeast Spo13. Therefore, it is reasonable to consider that the regulatory mechanisms of meiosis I specific kinetochore functions are conserved from yeast to mammals.

Published paper

Kim J.*, Ishiguro K.*, Nambu A., Akiyoshi B., Yokobayashi S., Kagami A., Ishiguro T., Pendas A. M., Takeda N., Sakakibara Y., Kitajima T. S., Tanno Y., Sakuno T. and Watanabe Y.

(*equal contribution)

“ Meikin is a conserved regulator of meiosis I specific kinetochore function.”

Nature 517, 466-71 (2015).

INTRODUCTION

1. Chromosome dynamics in mitosis and meiosis

Eukaryotic cells undergo two distinct types of cell division, mitosis and meiosis. In mitosis, sister chromatids (a pair of replicated chromosomes) are captured by microtubules originating from opposite poles (bi-orientation) at the kinetochore, and are divided equally into two diploid cells (equational division) (Fig. 1a). For this process to be successful, the association of sister chromatids (sister chromatid cohesion), which is mediated by Rad21-cohesin complexes, must be preserved until metaphase. At the onset of anaphase, cohesin complexes are removed completely along the entire chromosome length, triggering equational chromosome segregation (Fig. 1a).

Meiosis is a specialized cell cycle to reduce the chromosome number and generate haploid gametes. In meiosis, one round of DNA replication is followed by two sequential rounds of chromosome segregation (meiosis I and II). (Fig. 1b) (Uhlmann et al., 1999; Peters et al., 2008; Nasmyth & Haering, 2009). Therefore, the chromosome dynamics in meiosis differ in many ways from those of mitosis. Especially, three unique events are important for proper chromosome segregation during the first division of meiosis (meiosis I) (Fig. 1b). First, homologous chromosomes are connected by recombination structures (chiasmata) during meiotic prophase, thereby forming bivalents. Second, sister kinetochores (kinetochores of sister chromatids) are tightly fused and captured by microtubules originating from the same spindle pole in metaphase I (mono-orientation). Third, in anaphase I, sister chromatid cohesion, which is mediated by Rec8-cohesin complexes, is preserved at the centromere while it is lost along the chromosome arms, (centromeric cohesion protection). These mechanisms allow homologous chromosomes to separate to opposite poles while replicated sister chromatids move to the same

pole during meiosis I (reductional division) (Fig. 1b). Sister chromatids therefore stay connected until metaphase II when they can be properly aligned on the metaphase II spindle, and undergo equational segregation at anaphase II (Fig. 1b) (Moore and Orr-Weaver, 1998; Petronczki et al., 2003; Watanabe, 2012).

2. Cohesion in mitosis and meiosis

In both mitosis and meiosis, sister chromatid cohesion is established during DNA replication by a multi-protein complex called cohesin (Nasmyth & Haering, 2005). The mitotic cohesin complex contains four core subunits: two subunits of the structural maintenance of chromosomes (SMC) protein family (Smc1 and Smc3) and non-SMC subunits (stromal antigen (SA)1/2 and kleisin RAD21) (Uhlmann, 2009; Nasmyth & Haering, 2009).

Cohesin complexes are largely modified in meiosis. The most common modification is that RAD21 is replaced by a meiotic counterpart, REC8 (Watanabe, 2004). Other meiosis-specific cohesin subunits (RAD21L/COH-3/COH-4, SA3/Rec11 and SMC1β) are also expressed and act in meiosis in various organisms (Prieto et al., 2001; Revenkova et al., 2001; Kitajima et al., 2003; Severson et al., 2009; Ishiguro et al., 2011; Llano et al, 2012; Ishiguro et al., 2014). In addition to mediating sister chromatid cohesion, meiotic cohesin complexes regulate several chromosomal events during meiosis including synaptonemal complex formation, reciprocal recombination, mono-orientation of sister kinetochores and protection of centromeric cohesion throughout anaphase I (Ishiguro and Watanabe, 2007; Sakuno and Watanabe, 2009; Tachibana-Konwalski et al., 2013).

3. Protection of Centromeric cohesion during meiosis I

In mitosis, sister chromatid cohesion is established in S phase, and preserved until metaphase when the sister chromatids are captured by spindle microtubules from opposite poles and aligned on the spindle equator by the balance of poleward pulling forces and sister chromatid cohesion. At the onset of anaphase, the anaphase-promoting complex (APC) is activated to degrade securin, an inhibitory chaperone for separase that cleaves RAD21-cohesin and removes cohesion along the entire chromosome. This removal of cohesin triggers sister chromatid separation and their segregation to opposite spindle poles (equational division) (Fig. 1a) (Uhlmann et al., 1999; Peters et al, 2008; Nasmyth and Haering, 2009).

In meiosis, REC8 largely replaces RAD21, and is removed along the chromosome arms at anaphase I. In contrast, sister chromatid cohesion mediated by REC8 must be protected in the centromeres because cohesion at the centromeres is required to ensure equational division at meiosis II. A widely conserved protein family, shugoshin (SGO), which associates with protein phosphatase 2A (PP2A), plays a critical role in this protection of centromeric cohesion. Mammals have two shugoshin family proteins, SGO1 and SGO2 (Kitajima et al., 2004; Kitajima et al., 2006). Mouse SGO1 and SGO2 (mSGO1 and mSGO2) are expressed ubiquitously in both somatic and germ cells, but mSGO2 expression is remarkably strong in germ cells (Lee et al., 2008). Consistent with this fact, mSGO2 deletion leads to the loss of sister chromatid cohesion during anaphase I toward metaphase II, and results in random segregation in the following anaphase II (Fig. 3) (Lee et al., 2008; Llano et al., 2008). Notably, the mono-orientation of sister kinetochores, which is also an essential feature of meiosis I kinetochores, is not impaired in *SGO2* knockout mouse (Llano et al., 2008).

4. Monopolar attachment of sister kinetochores in meiosis I

During chromosome alignment in mitosis, sister chromatids are captured by spindle microtubules at kinetochores from opposite sides, a process called bipolar-attachment (Fig. 2a). Presumably, back-to-back assembly of sister kinetochores may facilitate bipolar-attachment in mitosis (Fig. 2c). In meiosis I, however, sister kinetochores are captured by microtubules originating from the same spindle pole, known as the monopolar-attachment (Fig. 2b). Monopolar-attachment of sister kinetochores is a conserved feature and an essential step for reductional division in meiosis I. Juxtaposition of the fusion of sister kinetochores might be important to facilitate monopolar-attachment (Fig. 2d).

Fission yeast Moa1 (Monopolar attachment protein 1) is a meiosis I specific kinetochore protein that regulates reductional chromosome segregation during meiosis I in fission yeast (Yokobayashi and Watanabe, 2005). Moa1 binds directly to Cnp3 (CENP-C, a widely conserved core component of centromeric chromatin) (Tanaka et al., 2009). Deletion of moa1 causes bi-orientation of sister kinetochores and equational chromosome segregation in meiosis I. Additionally, it has been suggested that Moa1 mediates cohesion to regulate the mono-orientation of sister kinetochores in meiosis I (Yokobayashi and Watanabe, 2005, Sakuno et al, 2009).

5. The purpose of this study

In meiosis I, there are two important forms of meiotic kinetochore regulation; first, sister kinetochores are captured by spindle microtubules emanating from the same pole

(mono-orientation), and second, centromeric cohesion is protected throughout anaphase I (cohesion protection). The precise regulation of sister kinetochores orientation and protection of sister chromatid cohesion are essential to ensure reductional chromosome segregation during meiosis I. Disorder in chromosome segregation during meiosis I might contribute to genomic instability and aneuploidy in humans.

So far, meiosis specific kinetochore proteins have been identified only in yeasts: fission yeast Moa1, and budding yeast Spo13 and Mam1 (monopolin subunit) (Hugerat and Simchen, 1993; Klapholz and Esposito, 1980; Toth et al., 2000, Katis et al., 2004; Lee et al., 2004; Yokobayashi and Watanabe, 2005). However, their homologs have remained unidentified in vertebrates including humans.

Fission yeast Moa1, by binding to Cnp3 (CENP-C), localizes to kinetochores in meiosis I and promotes mono-orientation and cohesion protection (Tanaka et al., 2009). Therefore, our laboratory (Dr. Aya Nambu) undertook yeast two hybrid screening from a mouse testis derived cDNA library to identify CENP-C interacting proteins, with the expectation of finding novel factors that regulate meiosis I kinetochore function, and to understand the kinetochore regulatory mechanism in mammalian meiosis.

RESULTS AND DISCUSSION

1. Mammalian meiotic kinetochore protein MEIKIN

1-1. Background

Although meiotic kinetochore regulators were studied in two yeasts (moa1 in fission yeast, Spo13 and mam1 in budding yeast) (Hugerat and Simchen, 1993; Klapholz and Esposito, 1980; Toth et al., 2000, Katis et al., 2004; Lee et al., 2004; Yokobayashi and Watanabe, 2005), the regulation of kinetochore function in mammals was a longstanding question because their homologs remained to be identified due to an apparent lack of amino acid sequence homology. Fission yeast moa1, a meiotic kinetochore regulator, associates directly with the conserved kinetochore protein Cnp3 (CENP-C homolog) and localizes to the kinetochore in meiosis I (Yokobayashi and Watanabe, 2005). To identify such meiosis-specific kinetochore factors in mammals, we performed yeast two-hybrid assays to search for proteins that interact with mouse CENP-C using a cDNA library prepared from mouse testis.

1-2. CENP-C interacting novel meiosis-specific protein *4930404A10rik*

Yeast two-hybrid screening for a mouse CENP-C interactor was performed by Dr. Nambu in our lab using the CENP-C C-terminus (a,a. 692-906) as bait from a mouse testis cDNA library. A total of 11.95 $x10^7$ colonies were screened on selective (SD-Trp-Leu-His-Ade, +10mM 3AT) plates using an AH109 tester strain. The list and number of isolated clones is summarized in (Fig. 4a). Next, looking for the meiosis-specificity of these genes, Dr. Nambu and Dr. Ishiguro examined their expression patterns by RT-PCR, and found that the expression of 4930404A10Rik is restricted to testis and ovary, indicating that its expression is germ cell-specific (Fig. 4b). Notably, *4930404A10Rik* is the most frequently obtained gene in

two-hybrid screening. To confirm the interaction between 4930404A10Rik and CENP-C *in vivo*, we prepared antibodies against MEIKIN (generated by Dr. Ishiguro), which Dr. Ishiguro used in immunoprecipitation assays using testis chromatin extracts to demonstrate that 4930404A10Rik indeed forms a complex with mCENP-C (Fig. 4c). We named this CENP-C interactor 4930404A10Rik MEIKIN (Meiosis-specific kinetochore protein) following an analysis of its localization and function (see below).

1-3. MEIKIN (*4930404A10Rik*) localizes to kinetochores during meiosis I

To investigate the localization of MEIKIN, spermatocytes were immunostained for the meiotic marker SYCP3, a component of the axial element, and the centromeric marker ACA (anti-centromeric antibodies), which stains constitutive centromeric proteins including CENP-C. MEIKIN begins to localize at kinetochores from pachytene when homologous chromosomes (homologs) are paired and synapsed, and reaches a peak in diplotene when homologs are desynapsed. After the breakdown of the nuclear envelope, MEIKIN signals decrease gradually until metaphase I, and finally disappear in anaphase I (Fig. 5a). There is an obvious contrast between the MEIKIN signal and ACA (or CENP-C), which increases gradually throughout meiosis I, and persists throughout meiosis II (Fig. 5a, c), suggesting that the interaction between MEIKIN and CENP-C is regulated in a meiosis I-specific manner. The MEIKIN localization pattern is similar in oocytes (Fig. 6a, b). MEIKIN shows no sequence similarity to fission yeast Moa1, but blast search analysis revealed MEIKIN to be a novel protein largely conserved among vertebrates including humans (Fig. 7). Collectively, we conclude that MEIKIN is a meiosis I-specific novel kinetochore protein in vertebrates.

1-4. MEIKIN C-terminus is important for the interaction with CENP-C

To elucidate the mechanism of MEIKIN localization, we performed yeast two-hybrid assays to find the minimum domain of MEIKIN needed to bind with CENP-C. We found that the MEIKIN c-terminus (a.a. 385-425 and a.a. 385-434) is an essential region for its interaction with CENP-C (Fig. 8a). To explain the precise localization mechanism of MEIKIN, we examined the ectopic expression of GFP-tagged MEIKIN in testis. Although yeast two hybrid assays indicate that MEIKIN a.a. 385-425 interacts with CENP-C, GFP-tagged MEIKIN expression revealed that this fragment does not localize to centromeres (Fig. 8b, d). These results suggest that the MEIKIN c-terminus a,a. 385-434 is the minimum domain for targeting to centromeres. To delineate the amino acid sequence required for MEIKIN localization, we generated alanine substitutions (5A and 4A) in the most highly conserved sequences of the MEIKIN C-terminus (Fig. 7, Fig. 8c). Indeed these mutations abolished centromeric localization in spermatocytes (Fig. 8b, d), confirming that the conserved sequences of the MEIKIN C-terminus play an essential role in targeting to kinetochores.

1-5. Conclusion

We performed yeast two hybrid screening to identify meiotic proteins that interact with CENP-C from a mouse testis cDNA library. The most frequently obtained clones (*4930404A10Rik* gene) encode a novel protein, which we termed MEIKIN (Meiosis-specific kinetochore protein). MEIKIN shows specific expression in germ cells and localizes to kinetochores during meiosis I, but never appears in meiosis II or mitosis. MEIKIN is widely

conserved among vertebrates, and conserved sequences in its C-terminus play an important role its localization to kinetochores. We conclude that MEIKIN is a novel meiotic kinetochore protein in mammals.

2. Generation of *Meikin* knockout (KO) mouse and its analysis

2-1. Background

To investigate MEIKIN function, we generated MEIKIN knockout (KO) mice. Because MEIKIN is expressed in the meiosis-specific organs (testis in males and ovary in females), we generated conventional (i.e. non-conditional) KO mice.

2-2. Targeting vector construction

The targeting vector was designed by Dr. Ishiguro to disrupt Exon 4 of the *Meikin* genomic locus (Fig. 9a). ES cells were transfected by electroporation of the targeting vector, then cultured (Baltha1 ES cells derived from C57BL/6N were used; mice in black coat color) (Kim-Kaneyama et al., 2011). G418-resistant ES clones were screened for homologous recombination with the *Meikin* locus by PCR, and confirmed by Southern blot of genomic DNA from wild type (+/+) and *Meikin* heterozygous (+/-) ES cells after Pvu II digestion. (Fig. 9a, b). Dr. Takeda of Kumamoto Univ. generated chimeric mice by blastocyst injection (host ICR; mice in white coat color) of recombinant ES cells (Kumamoto University, CARD). The obtained chimerism was determined by coat color (from 0% indicating all white color to 100% indicating all black color). We generated heterozygous mice by crossing chimera (70~100%) male mice with wild-type C57Bl/6N female mice. The obtained pups were genotyped by PCR of the genomic DNA, and their phenotypes were represented as wild-type (*Meikin*$^{+/+}$), heterozygous (*Meikin*$^{+/-}$) and homozygous (*Meikin*$^{-/-}$) mice. Both the MEIKIN protein and mRNA were successfully depleted in *Meikin*$^{-/-}$ (Fig. 9c, d). Immunostaining confirmed the absence of MEIKIN proteins from the kinetochores of *Meikin*$^{-/-}$ diplotene spermatocytes (Fig. 9e). In the

present study, each knockout animal was compared with littermates or age-matched non-littermates from the same colony. We used female mice age 1-3 months for the analysis.

2-3. *Meikin* KO mice are infertile

Although homozygous *Meikin*$^{-/-}$ mice develop normally and exhibit no obvious phenotype in growth, both male and female KO (knockout) mice are completely infertile because no offspring were produced when *Meikin*$^{-/-}$ male or female mice were mated with wild type mice over a period of 1 year. The same wild-type mice produced offspring when mated with *Meikin*$^{+/-}$ mice. In order to address the cause of infertility, we performed a histopathological analysis of the reproductive organs. The testes of *Meikin*$^{-/-}$ are almost the same size as those of their wild-type littermates (Fig. 10a). Also, the histological observations of *Meikin*$^{-/-}$ testes revealed that the organization and number of germ cells within the seminiferous tubules are normal (Fig. 10b), although the number of mature sperm is greatly reduced in the epididymis of *Meikin*$^{-/-}$ (Fig. 10b). In *Meikin*$^{-/-}$ females, no histological abnormalities of the ovaries were observed as compared to their wild-type littermates (Fig. 10d, e). The number of fully-grown GV oocytes is similar between wild-type and *Meikin*$^{-/-}$ following super ovulation treatment by PMSG; the average number of GV oocytes was 23 in WT (n = 7) and 22.6 in *Meikin*$^{-/-}$, (n = 5), (4-8 week-old female mice), implying that prophase progression is normal.

Intriguingly, however, we detected an approximately 2-fold increase in the kinetochore number in round spermatids, post meiosis cells, with enlarged nuclear size (Fig. 10f). These data suggest the possibility of meiotic cell division failure. Accordingly, immunostaining of male spermatocytes revealed apparently normal meiotic prophase progression as represented by

normal features of axial elements (AEs) formation, homologous chromosome (homologs) pairing, synapsis of homologs, chiasmata formation and chromosome condensation (Fig 9e, see below).

When the cell populations of wild-type and *Meikin*$^{-/-}$ (8 week-old) testes were subjected to FACS analysis (Fig. 10g), the cells prepared from wild-type testis showed a sharp peak at 1N, indicative of haploid spermatids, while those from *Meikin*$^{-/-}$ testis showed a significant decrease in the peak at 1N, and instead an increase at 2N, suggesting an impairment in the second meiotic division in *Meikin*$^{-/-}$. Therefore, we assume that meiotic cell division defects cause infertility, at least in male *Meikin*$^{-/-}$.

Taken together, both male and female *Meikin*$^{-/-}$ mice are infertile, but the histological analysis of testes and ovaries detected no obvious differences between wild-type and *Meikin*$^{-/-}$ mice.

2-4. MEIKIN is required for the protection of centromeric cohesion

In order to investigate the cause of infertility in *Meikin*$^{-/-}$, we carefully examined the progression of meiosis I in oocytes. By puncturing ovaries, we isolated fully grown GV oocytes (G2 phase) surrounded by cumulus cells. In culture medium, GV oocytes undergo germinal vesicle breakdown (GVBD) to resume meiosis I (M phase). When all bivalents, physically linked by chiasmata, are aligned and come under tension, the chiasmata are resolved by the separase-mediated dissociation of cohesion, and the homologs segregate to opposite poles (Fig. 1) (Kudo et al., 2006). In meiosis I, mouse oocytes extrude an asymmetrically sized glob of cytoplasm containing the halved chromosomes, called the first polar body (1st PB). Therefore,

the 1st PB extrusion indicates the progression of meiosis I cell division.

Light microscopic observation revealed that *Meikin*$^{-/-}$ oocytes extrude the 1st PB on average 2 h later than oocytes from wild-type littermates, although most mutant oocytes (>90%) eventually progress to anaphase I (Fig. 11a). While bivalents are tightly aligned at the spindle equator by 6 h after GVBD in wild-type, Meikin−/− oocytes show a loose alignment of bivalents (Fig. 11b). In order to examine the reason for the meiotic cell cycle delay in *Meikin*$^{-/-}$, we treated oocytes with Reversine (inhibitor of the SAC component Mps1 kinase), which inactivates the spindle assembly checkpoint (SAC). In *Meikin*$^{-/-}$ oocytes, the delay in the onset of anaphase was canceled by SAC inactivation (Fig. 11c). These data suggest that chromosome alignment defects and the consequent activation of the SAC might be the reason for the delay in the onset of anaphase I in *Meikin*$^{-/-}$ oocytes.

To analyze the spatiotemporal dynamics of kinetochores and chromosomes during meiosis I in live oocytes, Drs. Kitajima and Sakakibara (RIKEN CDB) recorded four-dimensional (4D) datasets of kinetochores and chromosomes, labeled as 2mEGFP-CENP-C and Histone 2B (H2B)-mCherry, respectively. (Kitajima et al., 2011). We followed the frames of live cell imaging at the onset of anaphase in both wild-type and *Meikin*$^{-/-}$ oocytes, and confirmed that loosely aligned bivalents in *Meikin*$^{-/-}$indeed segregate normally during anaphase I (Fig. 11d). Surprisingly, however, we detected that many pairs of sister kinetochores start to split at the onset of anaphase in *Meikin*$^{-/-}$oocytes, but that this is rare in wild-type oocytes (Fig. 11d). Live cell imaging of oocytes further revealed that chromosomes are significantly misaligned in metaphase II in *Meikin*$^{-/-}$ oocytes (Fig. 11e), presumably because sister chromatids are prematurely separated in anaphase I.

To determine the cause of premature sister chromatid separation in *Meikin*$^{-/-}$, we examined REC8 cohesin, which mediates cohesion in meiosis. Because Shugoshin-2 (SGO2) protects centromeric REC8 during meiosis I, we compared REC8 in *Sgo2*$^{-/-}$ (Lee et al., 2008; Llano et al., 2008). The initial localization of REC8 (and cohesion) to the inter-chromatid axis on metaphase I bivalents appears normal in all oocytes (Fig. 11f); however, centromeric REC8 signals are lost from metaphase II univalents in *Meikin*$^{-/-}$ oocytes as observed in *Sgo2*$^{-/-}$ oocytes.

These results raise the question of whether MEIKIN regulates SGO2. Therefore, we performed immunostaining of SGO2, which usually appears at centromeres, on metaphase I bivalents (Lee et al., 2008; Llano et al., 2008), and found, to our surprise, that SGO2 localization is decreased in *Meikin*$^{-/-}$ oocytes (Fig. 11g), suggesting that the impaired protection of centromeric cohesion might be caused by aberrant SGO2 localization in anaphase I. Similar defects were observed in *Meikin*$^{-/-}$ spermatocytes (Fig. 12a). Notably, the separation of sister kinetochores during anaphase I is less severe in *Meikin*$^{-/-}$ spermatocytes than in *Sgo2*$^{-/-}$ spermatocytes (Fig. 12b), indicating that the protection defects caused by *Meikin*$^{-/-}$ are somewhat milder than those by *Sgo2*$^{-/-}$.

In conclusion, *Meikin*$^{-/-}$ mice show premature sister chromatid separation during anaphase I and chromosome misalignment in metaphase II. Our experiments thus provide evidence that MEIKIN regulates the protection of REC8 cohesin during meiosis I, at least partially by stabilizing SGO2 localization.

2-5. MEIKIN facilitates mono-orientation

Because *Meikin*$^{-/-}$ oocytes show partially perturbed chromosome alignment during meiosis I (Fig. 11b), we postulated that the mono-orientation of sister kinetochores might also be impaired in mutant mice as in fission yeast *moa1*Δ cells (Yokobayashi and Watanabe, 2005). To further analyze the role of MEIKIN in mono-orientation, we measured the sister kinetochore distance of oocyte chromosomes in early prometaphase I when spindle microtubules rarely attach to the kinetochore. We fund that the distance between sister kinetochore pairs is increased (~20%) in *Meikin*$^{-/-}$ oocytes as compared with wild-type (Fig. 13a), and that similar defects are observed in *Meikin*$^{-/-}$ spermatocytes (Fig. 14a).

A previous study suggested that mono-orientation defects tend to be hidden by chiasmata (or tension between homologs, which mediates the bias to the bi-orientation of bivalents rather than univalents) during chromosome alignment (Yokobayashi and Watanabe, 2005; Shonn et al., 2002). We, therefore, examined chromosome alignment by deleting MEIKIN in an *Mlh1*$^{-/-}$ background. Because homologous chromosomes are not linked by chiasmata in *Mlh1*$^{-/-}$, meiosis I cells accumulate univalents that fail to align on the metaphase I plate and largely inhibit the onset of anaphase I (Fig. 13b) (Woods et al., 1999), presumably because tightly fused sister kinetochores prevent the bi-orientation of univalents. Interestingly, the further elimination of MEIKIN in an *Mlh1*$^{-/-}$ background reduced meiosis I arrest (Fig. 13b) despite the fact that *Meikin*$^{-/-}$ delayed anaphase onset in an *Mlh1*$^{+/+}$ background (Fig. 13b). We then carefully examined chromosome alignment 10 h after GVBD when most *Mlh1*$^{-/-}$ or *Mlh1*$^{-/-}$ *Meikin*$^{-/-}$ oocytes have not yet entered anaphase I. The number of bi-oriented sister kinetochores was determined by the sister kinetochore distance > 0.6 μm with a horizontal angle (0-10°) at the spindle midzone (10 μm width centered between spindle poles). For quantification, we only

used spindles up to 30 μm in length. Moreover, we used all single and double knockout mice in a C57BL/6 background in order to exclude the genetic differences among mouse strains (Nagaoka et al., 2011). Strikingly, approximately 50 % of univalents were aligned and bi-oriented on the metaphase I spindle equator in *Mlh1*$^{-/-}$ *Meikin*$^{-/-}$ oocytes, whereas only 10% bi-orientation was observed in *Mlh1*$^{-/-}$ oocytes (Fig. 13c). In contrast, *Mlh1*$^{-/-}$ *Sgo2*$^{-/-}$ oocytes showed no increase in the bi-orientation of univalents (Fig. 13c) indicating that a loss of cohesion protection is not the reason for the bi-orientation of univalents in *Mlh1*$^{-/-}$ *Meikin*$^{-/-}$. Also, a similar bi-orientation and alignment of univalents was observed in *Mlh1*$^{-/-}$ *Meikin*$^{-/-}$ spermatocytes (Fig. 14b).

Therefore, we conclude that MEIKIN plays a crucial role in mono-orientation in addition to the protection of centromeric cohesion.

2-6. Conclusion

We identified a meiosis-specific novel kinetochore protein, MEIKIN, in mouse, and found that both male and female *Meikin*$^{-/-}$mice are infertile. MEIKIN plays a role in protecting REC8 cohesin partly by stabilizing the localization of cohesin protector SGO2 in meiosis I. In addition, MEIKIN plays a crucial role in mono-orientation. We conclude that MEIKIN regulates two important kinetochore functions in meiosis I: cohesion protection and mono-orientation.

3. MEIKIN-PLK1 regulates cohesion protection and mono-orientation

3-1. Background

As found in our previous study, fission yeast moa1 recruits plo1 (Polo-like kinase, PLK1 in fission yeast) to the kinetochore, and the enriched Plo1 plays a crucial role in mono-orientation and cohesion protection in meiosis I. Therefore, in order to address the molecular function of MEIKIN, we searched for MEIKIN interactors.

3-2. MEIKIN recruits PLK1

To elucidate the molecular function of MEIKIN, Dr. Nambu in our lab performed yeast two-hybrid screening using the MEIKIN C-terminus (a.a. 272-434) as bait of a mouse testis cDNA library to search for MEIKIN interactors. Also, Dr. Ishigruo in our lab performed immunoprecipitation-MASS spectrometry of mouse testis chromatin extracts to find MEIKIN binding proteins. In both assays, we obtained Polo-like kinase PLK1 as a MEIKIN binding factor in addition to CENP-C (Fig. 15a), as with fission yeast moa1. Dr. Ishiguro confirmed that MEIKIN forms a complex with PLK1 *in vivo* using testis chromatin extracts (Fig. 15b).

Next we examined the localization of PLK1in mouse meiotic cells. Immunostaining spermatocytes revealed that PLK1 signals start to localize to the kinetochore from diplotene (end of prophase), reach a peak at metaphase I, and decline during anaphase I when MEIKIN disappears from the kinetochore. In metaphase II, PLK1 signals are prominent at the centrosome, suggesting that PLK1 enrichment at the kinetochore is meiosis I-specific. Surprisingly, PLK1 signals largely disappear from the kinetochores during meiosis I in *Meikin*$^{-/-}$ spermatocytes (Fig. 15c) indicating that PLK1 enrichment is dependent on MEIKIN during meiosis I. Similarly,

there is a decrease in PLK1 signals at kinetochores in *Meikin*$^{-/-}$ oocytes as well, although less than in spermatocytes (Fig. 15d). We measured and quantified CENP-U phosphorylation (a canonical PLK substrate, but not a MEIKIN-PLK specific substrate) in meiosis I spermatocytes and oocytes, and found that the phosphorylation is comparable to the protein level of PLK rather than MEIKIN (Fig. 15e, f), implying that MEIKIN-independent PLK1 exists in *Meikin*$^{-/-}$ oocytes. Taken together, MEIKIN recruits PLK1 to kinetochores during meiosis I, suggesting that enriched PLK1 activity dependent on MEIKIN might be required for kinetochore regulation in meiosis I.

3-3. PLK1 activity is required for cohesion protection and mono-orientation

In order to examine the functions of PLK1 in meiosis I, we inhibited PLK1 activity in an oocyte culture by adding BI 2536, a potent and selective inhibitor of PLK1 (Lenart et al., 2007). Because long-term treatment of oocytes cultures with BI 2536 interferes with the progression of meiosis I and 1st PB extrusion, we tried a 2 h transient BI 2536 treatment of a meiosis I oocyte culture (Fig. 16a). We added BI 2536 for 2 h beginning 4 h after GVBD because this timing would allow the 1st PB extrusion to have taken place in approximately 70% of oocytes, and suppress PLK1 activity at the kinetochores (Fig. 16a, b). Additionally, when we treated spermatocytes with BI 2536, MEIKIN signals increased in metaphase I (Fig. 16c), suggesting that MEIKIN dissociation from the kinetochores is accelerated by PLK1 activity. Taken together, the transient addition of BI 2536 to oocytes cultures overcomes the arrest of meiotic division while effectively suppressing PLK1 activity at the kinetochore, and, at least, does not reduce MEIKIN localization in meiosis I.

We tested the requirement of PLK1 activity for cohesion protection in meiosis I. Oocyte cultures were treated with BI 2536 for 2 h (4-6 h post GFVD), and examined for chromosome alignment at 20 h (note that oocytes usually arrest in metaphase II) (Fig. 17a). Oocytes treated with BI 2536 during prometaphase I progress to anaphase I normally, but sister chromatids separate prematurely at the onset of anaphase I (Fig. 17a). Surprisingly, more than 50% of BI 2536-treated oocytes showed chromosome misalignment in metaphase II, presumably because the premature loss of cohesion during anaphase I causes sister chromatid separation and misalignment in metaphase II (Fig. 17a). To test this possibility further, we measured REC8 cohesin signals in spread chromosomes at metaphase II. Indeed, centromeric REC8 was found to be largely decreased in BI 2536-treated metaphase II oocytes (Fig. 17b). These results suggest that PLK1 activity plays an important role in protecting centromeric REC8 during meiosis I.

To address whether Plk1 is also required for the mono-orientation of sister kinetochores in meiosis I, we analyzed *Mlh1*$^{-/-}$ oocytes treated with BI 2536 for one hour between 9 h – 10 h after GVBD when *Mlh1*$^{-/-}$ oocytes are usually arrested in metaphase I. Intriguingly, whereas univalents failed to align in *Mlh1*$^{-/-}$ oocytes, BI 2536 treated *Mlh1*$^{-/-}$ oocytes showed significantly increased bi-orientation of univalents on the metaphase I plate (Fig. 17c). These data suggest that PLK1 activity is also required for mono-orientation in oocytes during meiosis I.

3-4. Conclusion

We identified PLK1 as a binding partner of MEIKIN, and showed that PLK1 accumulates to

kinetochores dependent on MEIKIN in meiosis I. We confirmed that PLK1 activity is required for cohesion protection and mono-orientation of sister kinetochores during meiosis I. We, therefore, assume that MEIKIN regulates two important functions of kinetochores during meiosis I, cohesion protection and mono-orientation, partly by enriching PLK1.

OVERALL CONCLUSION

Here we identified a meiosis-specific kinetochore protein, MEIKIN, in mouse that plays a crucial role in meiosis I. MEIKIN regulates two important functions of the meiotic kinetochore, mono-orientation and cohesion protection. (Fig. 18a-b) These functions are facilitated by the activity of Polo-like kinase PLK1, which is enriched at the kinetochore in a MEIKIN-dependent manner (Fig. 18c).

We took advantage of our previous study showing that fission yeast Moa1 interacts directly with Cnp3 (CENP-C) (Tanaka et al., 2009) even though there is no significant homology between the sequences of MEIKIN and Moa1. However, the current study, together with parallel studies using fission yeast performed by other members of our laboratory, revealed, first, that MEIKIN C-terminus domains are essential for kinetochore localization by binding directly to CENP-C, as in the case of Moa1. Second, MEIKIN regulates mono-orientation and cohesion protection during meiosis I, as in the case of Moa1 (Yokobayashi and Watanabe, 2005). Third, MEIKIN recruits PLK1 to the kinetochore, and that the enriched PLK1 (PLK1 activity) plays a crucial role in mono-orientation and cohesion protection in meiosis I, also as in the case of Moa1 (Fig. 15 c,d, Fig. 17). Because of these biochemical and functional similarities, we conclude that MEIKIN is a functional homologue of Moa1 (Fig. 18d). Further, it turns out that Spo13, a meiotic kinetochore protein in budding yeast that regulates mono-orientation and cohesion protection (Shonn et al., 2002; Lee et al., 2002; Katis et al., 2004; Lee et al., 2004; Matos et al., 2008) shares some of the properties of MEIKIN and Moa1. Taken together, these results suggest that MEIKIN, Moa1 and Spo13 are functional homologues in regulating meiotic kinetochore functions in meiosis I (Fig. 18d).

Meiosis is a specialized cell cycle to allow the halving of the number of chromosomes through two rounds of cell division. To accomplish the specialized chromosome segregation in meiosis, sister kinetochores are mono-oriented and centromeric cohesion is protected throughout meiosis I. Notably, defects in the first meiotic cell division are the leading cause of miscarriage and genetic disorders such as Down syndrome in humans (Hassold and Hunt, 2001). Accumulating evidence suggests that meiosis I chromosomes in aged mouse oocytes show defects in sister chromatid cohesion (or REC8 maintenance), which would increase the number of chromosome segregation errors in the following meiotic divisions (Hodges et al., 2005; Lister et al., 2010; Chiang et al., 2010; Jessberger., 2012).

Up to now, meiotic kinetochore factors required for mono-orientation and cohesion protection in meiosis I have been identified only in yeasts (Watanabe., 2012); however, this study identified a meiosis I-specific kinetochore regulator, MEIKIN, in mouse that is conserved among vertebrates including humans. Our study demonstrates the appearance of MEIKIN at kinetochores in prophase I (the fetal period in females), and its persistence during metaphase I (several months after birth in adult female mice) (Fig. 6). These results suggest that MEIKIN must be maintained at kinetochores beyond several months until ovulation in female mice. Therefore, it is possible that MEIKIN might be a factor in age-associated chromosome segregation disorders, a major cause of human birth defects, although further research of MEIKIN in aged oocytes is required (Hassold and Hunt, 2001).

Material and Methods

Yeast two-hybrid screening and assay

For yeast two-hybrid screening, mouse *CENP-C* cDNA encoding the C-terminus (a.a. 692-906) and mouse *Meikin* cDNA encoding the C-terminus (a.a. 272-434) were subcloned into the vector pGBKT7. The bait strains were raised by transforming the bait vector into the yeast strain AH109. A matchmaker mouse testis cDNA library (Clontech) was transformed into the bait strains, and positive transformants were selected on nutrition-restricted plates (SD-trp-leu-his-ade, +10mM 3AT). Positive transformants were further examined by blue/white assay to confirm the interaction. Prey plasmids were extracted from the candidate clones and sequenced. To exclude false positive clones, the candidate prey plasmids were retransformed into the yeast strain AH109 along with the bait vector or negative control bait vector of p53.

For yeast two-hybrid assays, the following cDNAs were subcloned into the bait vector pGBKT7: hCENP-C full length, hCENP-C C-terminal region (a.a. 732-945), mPLK1 full length, hPLK1 full length. The following cDNAs were subcloned into prey vector pACT2: MEIKIN full length, MEIKIN N-terminus (a.a. 1-271), MEIKIN C-terminus (a.a. 272-434), MEIKIN Ex1-12 (a.a. 1-384), MEIKIN Ex 13-14 (a.a. 385-434). The following cDNAs were subcloned into the prey vector pGADT7: hMEIKIN N-terminus (a.a. 1-264), hMEIKIN C-terminus (a.a. 259-373). These bait and prey preparations were co-transformed into the yeast strain AH109.

Mice

Sgo2- and *Mlh1*^{tm1Liskay}- knockout mice were reported earlier (Llano et al., 2008; Baker et al.,

1996). All single and double knockout mice were congenic with the C57BL/6 background. Whenever possible and unless indicated otherwise, each knockout animal was compared to littermates or age-matched non-littermates from the same colony. Animal experiments were approved by the Institutional Animal Care and Use Committee (approval #23001, #23013, #24001, #25012) at IMCB and AH23-05-04 at CDB).

Generation of *Meikin* (*4930404A10Rik*) knockout mouse and genotyping

The targeting vector was designed to disrupt Exon 4 of the *Meikin* genomic locus. Targeting arms of 4.40 kb and 4.98 kb fragments, 5' and 3' to Exon 4 of the *Meikin* gene, respectively, were generated by PCR from mouse C57BL/6 BAC clone (RPCI23-32I13), and cloned directionally flanking the p*GK-Neo*-polyA and *DT-A* cassettes. Homologous recombinant cells were isolated using Baltha1 ES cells derived from C57BL/6N (Kim-Kaneyama et al., 2011), and chimeric mice were generated by morula injection (host ICR) of recombinant ES cells (Kumamoto university, CARD). The G418-resistant ES clones were screened for homologous recombination with the *Meikin* locus using PCR primers:

MEIKIN-7547F : 5'-GTTCAGTTTCACCTCCCGGTCTGAC and

Neo3R: 5'-TACCGGTGGATGTGGAATGTGTGC for the left arm (4734 bp),

Neo104F : 5'-ggaccgctatcaggacatagcgttggc and

MEIKIN-18860R: 5'-ACTCGCCACTGACTTCTCCTGTGAGC for the right arm (5531bp).

The correct targeting of the ES cell clones was confirmed by Southern blot: DNA was digested with Pvu II for Southern blots with an external 5'-probe. Chimeric males were mated to C57BL/6 females and the progeny were genotyped by PCR using the following primers. Ex3F

(common-forward): 5’- CCCCAGAGGAAAAGACACCACC-3’, Ex4R (wild-type-reverse): 5’-CTCGACAACAAGCTGTCCATCTC-3’ and Neo4R (mutant-reverse): 5’-CATGAGTGGGAGGAATGAGCTGGC-3’ for the *Meikin* mutant allele (3473 bp) and the wild-type allele (1750 bp).

Histological analyses

The testes, epididymides or ovaries from mice (12-week-old males, 8-week-old females) were fixed in Bouin's solution and embedded in paraffin. Sections 5 μm in thickness were prepared on APS-coated slides (Matsunami), and the slides were dehydrated and stained with hematoxylin and eosin.

FACS analysis

Preparation of cells from testis and FACS analysis were done as described previously (Ishiguro et al. 2014). Briefly, seminiferous tubules from wild-type and mutants (8 weeks old) were minced and digested with 100 μg/ml collagenase for 30 min and 100 U/ml DNase I (Takara) for 15 min at 34ºC followed by filtration through a 40 μm cell strainer (FALCON). The testicular cells were fixed in 70% ethanol and brought to a concentration of 1-2 x 10^6 cells/ml in propidium iodide/RNase solution (BD Biosciences 550825). Cells were analyzed by a FACSort instrument equipped with an argon laser a (Becton, Dickinson). A total of 50,000 cells were counted.

Antibody production

Polyclonal antibodies against mouse MEIKIN (a.a. 1-434) and MEIKIN C-terminal (a.a. 317-434) were generated by immunizing rabbits and mice. Polyclonal antibodies against human MEIKIN N- and C-terminal regions were generated by immunizing ICR mice. All His-tagged recombinant proteins were produced by inserting cDNA fragments in-frame with pET19b or pET28c (Novagen). All His-tagged recombinant proteins were purified by Ni-NTA (QIAGEN) under denaturing conditions using 6 M Guanidine-HCl. The antibodies were affinity-purified from the immunized serum with immobilized peptides on CNBr-activated Sepharose (GE Healthcare).

Antibodies

The following primary antibodies were used for immunoblot (IB) and immunofluorescence (IF) studies: mouse anti-tubulin (IB, 1:5000, IF, 1:1000, DM1A, Sigma, Cat#T9026), human ACA (IF, 1:20, MBL, Cat#NA-8184), mouse anti-PLK1 (IB and IF, 1:1000, Abcam, Cat#ab17056), rabbit anti-CENP-U/MLF1 phosphoT78 (IF, 1:100, Abcam, Cat#ab34911), rabbit anti-Histone H3 (IB, 1:1000, Abcam, Cat#ab1791), rabbit anti-GFP (IF, 1:1000, Invitrogen, Cat#A11122). The following polyclonal antibodies were described previously: rabbit anti-mCENP-C (IB and IF, 1:1000), rabbit anti-mREC8 (IF, 1:500), mouse anti-mREC8 (IF, 1:500), mouse anti-mSYCP3 (IF, 1:1000) (Ishiguro et al., 2011). Mouse anti-mSGO2 (IF, 1:500) (Kawashima et al., 2010), Rabbit anti-mSGO2 (IF, 1:1000) (Lee et al., 2008), Rat anti-mSYCP3 polyclonal antibody (IF, 1:1000) (Morimoto et al., 2012).

The following secondary antibodies were used for immunofluorescence studies:

Alexa488-conjugated donkey anti-mouse (Invitrogen, Cat#A21202), donkey anti-rabbit (Invitrogen, Cat#A21206), Alexa555-conjugated goat anti-mouse (Invitrogen, Cat#A21422), donkey anti-rabbit (Invitrogen, Cat#A31572), goat anti-human (Invitrogen, Cat#A21433), goat anti-rat (Invitrogen, Cat#A21434), Alexa647-conjugated donkey anti-mouse (Invitrogen, Cat#A31571), goat anti-rabbit (Invitrogen, Cat#A21244), goat anti-human (Invitrogen, Cat#A21445), goat anti-rat (Invitrogen, Cat#A21247).

***In vitro* oocyte culture**

Ovaries collected from 6 to 12-week-old female mice were used for this study 46 to 48 h after treatment with 5 IU of pregnant mare serum gonadotropin. GV oocytes were isolated by puncturing follicles in M2 medium (Sigma) containing 250 μM 3-isobutyl-1-metyl-xanthine (IBMX, Sigma) to maintain prophase arrest. To induce the resumption of meiosis, the oocytes were cultured in M16 medium (Sigma) supplemented with 10% FBS in a 5% CO_2 atmosphere at 37ºC. Oocytes that had not undergone GV breakdown (GVBD) by 90 min were removed from the experiment. For oocyte drug treatment, 100 nM BI 2536 (ChemieTek), 5 μM reversine (Sigma) and 10 μM nocodazole (Sigma) were added to the culture medium at the indicated time point; control oocytes were treated with an equivalent volume of DMSO.

Immunofluorescence microscopy of spermatocytes and oocytes

Squashed spermatocytes were prepared from adult male mice as described previously[12] with modification. Briefly, seminiferous tubules were minced and fixed in fixation buffer comprising 2% paraformaldehyde (PFA)/0.1% Triton X-100/PBS. The cell suspension was filtered through

a cell strainer (BD Falcon) to remove debris, pipetted repeatedly, and centrifuged. The cell pellets were suspended in fixation buffer and gently squashed with a cover glass. After fixation, the slides were frozen in liquid nitrogen. For immunostaining, the frozen slides were immersed in PBS and the coverslips were removed.

Fixed whole mount oocytes were prepared as described previously[11, 25] with minor modification. After *in vitro* culture, the oocytes were fixed in fixation buffer for 30 min at room temperature, washed with PBS, and then blocked with 3% BSA/PBT (0.1% Triton X-100/PBS) for 1 h at room temperature. For the measurement of sister kinetochore distance at early prometaphase I, oocytes were exposed to 1% Pronase (Sigma) to remove the zona pellucida, and fixed in fixation buffer on glass slides for 3 h.

Oocyte chromosome spreads were prepared as described previously (Chambon et al., 2013). Briefly, after the removal of the zona pellucida, oocytes were transferred onto glass slides and fixed in a solution of 1% PFA/0.15% Triton X-100/distilled H_2O adjusted to pH 9.2. After a quick dry, chromosomes were immunostained as described above. Fetal oocyte chromosome spreads were prepared as described previously (Hodges et al., 2002).

For immunostaining spermatocytes and oocytes, samples were washed briefly in PBS, blocked with 3% BSA/PBS for 10 min at room temperature, and incubated with primary antibodies in 3% BSA/PBS for 1 h and secondary antibodies for 1 h at room temperature. For whole mount oocytes, incubation was performed at 4^{o}C overnight for each antibody. The slides were washed

with PBS, and mounted using VECTASHIELD medium with DAPI (Vector Laboratories).

Images were acquired on an IX-70 microscope (Olympus) equipped with a CoolSnap HQ CCD camera (Roper Scientific), DeltaVision Core system (GE Healthcare). Only whole mount oocyte images were captured with an FV1000 confocal laser scanning microscope at 1 μm intervals and processed with FLUOVIEW software (Olympus).

Image projection, quantification of signal intensity, and measurement of sister kinetochore distance were carried out with the SoftWorx software program (GE Healthcare). For the measurement of sister kinetochore distance, images were acquired with Z-sections encompassing the entire nuclei. The peak-to-peak distance of CENP-C signals was measured for a pair of sister kinetochores in structurally preserved nuclei. The sister kinetochore distance was measured by calculating the square root of $X^2 + Y^2 + Z^2$.

Exogenous expression of GFP-tagged MEIKIN variants in testis

For the exogenous expression of GFP-tagged MEIKIN variants in testis, plasmid DNA was injected into live-mouse testes as described previously (Shibuya et al., 2014), and the *Meikin* variants were cloned in pCAG vector. Plasmid DNA was injected into live-mouse testes as described previously (Shibuya et al., 2014). Briefly, male mice 16-20 days postpartum were anesthetized with pentobarbital and the testes were pulled from the abdominal cavity. 50 μg of plasmid DNA (10 μl of 5 μg/μl DNA solution) was injected into each testis using glass capillaries under a stereomicroscope (M165C; Leica). The testes were held between a pair of

tweezer-type electrodes (CUY21; BEX), and electric pulses were applied four times and again four times in the reverse direction at 30 V for 50 ms each pulse. The testis was then returned to the abdominal cavity, and the abdominal wall and skin were closed with sutures. Immunostaining was performed 24-48 h after electroporation to assess the localization of the GFP-tagged MEIKIN variants in spermatocytes using rabbit anti-GFP (Invitrogen). Because the efficiency of GFP-tagged protein expression in meiotic prophase is 5-10%, we detected the kinetochore localization of GFP-tagged MEIKIN from GFP-positive cells.

Live confocal imaging of oocytes

Oocytes were microinjected with *in vitro*-transcribed RNAs encoding 2mEGFP-CENP-C (0.8 pg) and H2B-mCherry (0.2 pg), and incubated for 3 h before IBMX washout. The timing of GVBD was determined by low resolution time-lapse imaging. Oocytes not undergoing GVBD within 1.5 h after IBMX washout were removed from further imaging analysis. High resolution imaging was started around 5.5 h after GVBD. Imaging was performed with a Zeiss LSM710 equipped with a 40x C-Apochromat 1.2 W Corr M27 objective lens (Carl Zeiss) and a 3D multi-location tracking macro (Rabut et al., 2004). We acquired 17 z-confocal sections (every 1.5 μm) of 2-time-averaged 512 x 512 pixel xy images, which covered a volume of 30.36 μm x 30.36 μm x 25.5 μm at 5-min time intervals. 2mEGFP-CENP-C signals were peak-enhanced and background-subtracted as previously described[25]. The images were 3D-reconstructed with Imaris (Bitplane) and the kinetochore signals during anaphase were manually tracked. The kinetochore tracks were visualized by POV-Ray (www.povray.org).

PCR with reverse transcription

Total RNA was isolated from tissues using Trizol (Invitrogen). cDNA was generated from 0.5 μg of total RNA using Superscript III (Invitrogen) followed by PCR amplification using Ex-Taq polymerase (Takara) and template cDNA (derived from 1ng RNA equivalent). Sequences of the primers used to generate RT-PCR products from cDNA were as follows:

Meikin-F2 :5'-agatggacagcttgttgtcgagta-3';

Meikin k-R2 :5'-ctcagcaaatacaacctcagaagc-3';

GAPDH-F :5'-ttcaccaccatggagaaggc-3';

GAPDH-R :5'-ggcatggactgtggtcatga-3';

mSMC1-3516F:5'-ttacatcaaggaacagtcaacttgc-3';

mSMC1--3702R: 5'-ctattgttcattggggttggggttg-3';

Zfp438-F1:5'-gtatgcaaggacctgacaactcac-3';

Zfp438-R1:5'-catttgcttcctcctctctgtgta-3';

BC051142-F1:5'-ccttatcaaccttgtcagccttct-3';

BC051142-R1: 5'-ctcgaatctctttggacagcagta-3';

Nsun7-F1:5'-cctctcgatttaccatattctgcc-3';

Nsun7- R1: 5'-tatcaaagccttcacagagtggac-3';

Spesp1-F1:5' -catgaagctggtggtcctagttg-3';

Spesp1-R1:5' -gatggaccagaatgctgtactttg-3';

Snf1lk-F1:5' -gaggtccagctcatgaaacttttg-3';

Snf1lk-R1:5' -gctagcttgatatccatgttgctg-3';

Acbd3-F1:5' -caggagcagcactatcagcagtat

Acbd3-R1:5’ -cgacttctcctcgacgtactgtaa

Ncor1-F1:5’-aactcttctggtggaggtgactct-3’;

Ncor1-R1:5’-tgcccaggaataggagatttagac-3’;

Immunoprecipitation and mass spectrometry using testis extracts

Testis chromatin-bound and -unbound extracts were prepared and immunoprecipitated as described previously[53]. Briefly, immunoprecipitations were performed with protein A-Dynabeads (Invitrogen)-conjugated rabbit anti-mCENP-C, rabbit anti-MEIKIN and control rabbit IgG (5 μg equivalent) from the chromatin-bound fraction prepared from 40 - 60 wild-type testes (3 weeks-old). Co-immunoprecipitated proteins were subjected to electrophoresis in 4-12 % NuPAGE gels (Invitrogen) in MOPS-SDS buffer, and immunoblotted or analyzed by LC-MS/MS.

Fractions containing the MEIKIN immunoprecipitates were concentrated by precipitation with 10% trichloroacetic acid. The derived precipitates were dissolved in 7 M Urea, 50 mM Tris-HCl (pH 8.0), 5 mM EDTA solution containing 5 mM DTT at 37℃ for 30 min, and the cysteine SH groups were alkylated with 10 mM iodoacetamide at 37℃ for 1 h. Following alkylation, the solutions were desalted by methanol/chloroform precipitation, and the precipitates were dissolved in 2 M urea, 50 mM Tris-HCl buffer and subjected to trypsin gold (Promega) digestion overnight at 37℃. The resulting mixture of peptides was applied directly to the LC-MS/MS analysis system (Zaplous, AMR, Tokyo, Japan) using Finnigan LTQ mass spectrometry (Thermo Scientific) and a reverse phase C18 ESI column (0.2 x 50 mm, LC assist).

The protein annotation data were verified in mouse NCBI sequences using Bioworks software (Ver. 3.3; Thermo Scientific) with quantitation featuring the SEQUEST search algorithm.

Cloning of human *Meikin* homolog cDNA

Human *Meikin* homolog cDNAs encoding the N-terminus (a.a. 1-264) and C-terminus (a.a. 259-373) were cloned from a human testis cDNA library (Takara) using the following primer sets:

NheI-hMEIKIN-N-1F :tACCGGT gctagc atgtggccgctacgggtctataccc and

NotI-hMEIKIN-N-795R: tACtCGGTgcggCCgCttattctgcttcaatacttgctttttc for N-terminus,

NheI-hMEIKIN-C-1F: tACCGGTgctagcatgcagaaaacaaattccagtactc and

NotI-hMEIKIN-C-354R: tACtCGGTgcggCCgCtcatgccatttttattatgatatcttg for C-terminus.

Immunostaining of human seminiferous tubule sections

Frozen sections of adult human testis were purchased from Biochain. After washing with PBS/0.1% Triton X100, immunostaining was performed as described above.

References

Baker, S.M. *et al.* Involvement of mouse Mlh1 in DNA mismatch repair and meiotic crossing over. *Nat Genet* 13, 336-342 (1996).

Brar, G.A. & Amon, A. Emerging roles for centromeres in meiosis I chromosome segregation. *Nat Rev Genet* 9, 899-910 (2008)

Buonomo, S.B. *et al.* Disjunction of homologous chromosomes in meiosis I depends on proteolytic cleavage of the meiotic cohesin Rec8 by separin. *Cell* 103, 387-398. (2000).

Chiang, T., Duncan, F.E., Schindler, K., Schultz, R.M. & Lampson, M.A. Evidence that weakened centromere cohesion is a leading cause of age-related aneuploidy in oocytes. *Curr Biol* 20, 1522-1528 (2010).

Hassold, T. & Hunt, P. To err (meiotically) is human: the genesis of human aneuploidy. *Nat Rev Genet* 2, 280-291 (2001).

Dissociation of cohesin from chromosome arms and loss of arm cohesion during early mitosis depends on phosphorylation of SA2. *PLoS Biol.* 3: e69 (2005).

Hodges, C.A., Revenkova, E., Jessberger, R., Hassold, T.J. & Hunt, P.A. SMC1beta-deficient female mice provide evidence that cohesins are a missing link in age-related nondisjunction. *Nat Genet* 37, 1351-1355 (2005).

Hugerat, Y. & Simchen, G. Mixed segregation and recombination of chromosomes and YACs during single-division meiosis in spo13 strains of Saccharomyces cerevisiae. *Genetics* 135, 297-308 (1993).

Ishiguro, K. and Watanabe, Y. Chromosome cohesion in mitosis and meiosis. *J Cell Sci.* 120:367-9 (2007).

Ishiguro, K. *et al*. Meiosis-specific cohesin mediates homolog recognition in mouse spermatocytes. *Genes Dev.* 28:594-607 (2014).

Jessberger, R. Age-related aneuploidy through cohesion exhaustion. *EMBO Rep* 13, 539-546 (2012).

Katis, V.L. *et al.* Spo13 facilitates monopolin recruitment to kinetochores and regulates maintenance of centromeric cohesion during yeast meiosis. *Curr. Biol.* 14, 2183-2196 (2004).

Kim, J. et al., Meikin is a conserved regulator of meiosis I specific kinetochore function. *Nature* 517, 466-71 (2015).

Kim-Kaneyama, J.R. *et al.* Hic-5 deficiency enhances mechanosensitive apoptosis and modulates vascular remodeling. *J Mol Cell Cardiol* 50, 77-86 (2011).

Kitajima, T.S., Miyazaki, Y., Yamamoto, M. & Watanabe, Y. Rec8 cleavage by separase is required for meiotic nuclear divisions in fission yeast. *Embo J* 22, 5643-5653 (2003).

Kitajima TS. *et al*. Distinct cohesin complexes organize meiotic chromosome domains. science 300:1152-5 (2003)

Kitajima, T.S., Kawashima, S.A. & Watanabe, Y. The conserved kinetochore protein shugoshin protects centromeric cohesion during meiosis. *Nature* 427, 510-517 (2004).

Kitajima, T.S., Ohsugi, M. & Ellenberg, J. Complete kinetochore tracking reveals error-prone homologous chromosome biorientation in mammalian oocytes. *Cell* 146, 568-581 (2011).

Kitajima, T.S. *et al.* Shugoshin collaborates with protein phosphatase 2A to protect cohesin. *Nature* 441, 46-52 (2006).

Klapholz, S. & Esposito, R.E. Recombination and chromosome segregation during the single division meiosis in SPO12-1 and SPO13-1 diploids. *Genetics* 96, 589-611. (1980).

Kudo, N.R. *et al.* Resolution of chiasmata in oocytes requires separase-mediated proteolysis. *Cell.* 126:135-46 (2006).

Lee, J. *et al.* Unified mode of centromeric protection by shugoshin in mammalian oocytes and somatic cells. *Nature Cell Biol.* 10, 42-52 (2008).

Lee, B.H., Kiburz, B.M. & Amon, A. Spo13 maintains centromeric cohesion and kinetochore coorientation during meiosis I. *Curr. Biol.* 14, 2168-2182 (2004).

Lee, B.H., Amon, A. & Prinz, S. Spo13 regulates cohesin cleavage. *Genes Dev.* 16, 1672-1681. (2002).

Lenart, P. *et al.* The small-molecule inhibitor BI 2536 reveals novel insights into mitotic roles of polo-like kinase 1. *Curr Biol* 17, 304-315 (2007).

Lister, L.M. *et al.* Age-related meiotic segregation errors in mammalian oocytes are preceded by depletion of cohesin and Sgo2. *Curr Biol* 20, 1511-1521 (2010).

Llano, E. *et al.* A.M. Meiotic cohesin complexes are essential for the formation of the axial element in mice. *J Cell Biol.* 25: 877-85 (2012).

Matos, J. *et al.* Dbf4-dependent CDC7 kinase links DNA replication to the segregation of homologous chromosomes in meiosis I. *Cell* 135, 662-678 (2008).

Moore, D.P. & Orr-Weaver, T.L. Chromosome segregation during meiosis: building an unambivalent bivalent. *Curr Top Dev Biol* 37, 263-299 (1998).

Nagaoka, L.M. *et al.* Chromosomal influence on meiotic spindle assembly: abnormal meiosis I in female Mlh1 mutant mice. *J Cell Biol* 145, 1395-1406 (1999).

Nasmyth, K. & Haering, C.H. Cohesin: its roles and mechanisms. *Annu Rev Genet* 43, 525-558 (2009).

Nasmyth, K. & Haering, C. H. The structure and function of SMC and kleisin complexes. *Annu. Rev. Biochem.* 74, 595-648. (2005).

Nasmyth, K. Cohesin: a catenase with separate entry and exit gates? *Nature Cell Biol.* 13, 1170–1177 (2011).

Page, S.L. & Hawley, R.S. The genetics and molecular biology of the synaptonemal complex. *Annu Rev Cell Dev Biol.* 20: 525–558 (2004).

Peters, J.M., Tedeschi, A. & Schmitz, J. The cohesin complex and its roles in chromosome biology. *Genes Dev* 22, 3089-3114 (2008).

Petronczki, M., Siomos, M. F. & Nasmyth, K. Un menage a quatre: the molecular biology of chromosome segregation in meiosis. *Cell* 112, 423–440 (2003).

Prieto, I. *et al*. Mammalian STAG3 is a cohesin specific to sister chromatid arms in meiosis I. *Nat Cell Biol.* 3: 761–766 (2001).

Revenkova, E. *et al*. Novel meiosis‐specific isoform of mammalian SMC1. *Mol Cell Biol.* 21: 6984–6998 (2001).

Sakuno, T. & Watanabe, Y. Studies of meiosis disclose distinct roles of cohesion in the core centromere and pericentromeric regions. *Chromosome Res.* 17:239-49 (2009).

Severson AF. *et al*. The axial element protein HTP-3 promotes cohesin loading and meiotic axis assembly in C. elegans to implement the meiotic program of chromosome segregation. Genes Dev. 23:1763-78 (2009)

Shonn, M.A., McCarroll, R. & Murray, A.W. Spo13 protects meiotic cohesin at centromeres in meiosis I. *Genes Dev* 16, 1659-1671. (2002).

Tachibana-Konwalski, K. *et al.* Spindle assembly checkpoint of oocytes depends on a kinetochore structure determined by cohesin in meiosis I. *Curr Biol* 23, 2534-2539 (2013).

Tachibana-Konwalski, K. *et al.* Rec8-containing cohesin maintains bivalents without turnover during the growing phase of mouse oocytes. *Genes Dev* 24, 2505-2516 (2010).

Toth, A. *et al.* Functional genomics identifies monopolin: a kinetochore protein required for segregation of homologs during meiosis I. *Cell* 103, 1155-1168 (2000).

Uhlmann, F., Lottspeich, F. & Nasmyth, K. Sister-chromatid separation at anaphase onset is promoted by cleavage of the cohesin subunit Scc1. *Nature* 400, 37-42 (1999).

Uhlmann, F. A matter of choice: the establishment of sister chromatid cohesion. *EMBO Rep*. 10, 1095–1102 (2009).

Uhlmann, F. A matter of choice: the establishment of sister chromatid cohesion. *EMBO Rep*. 10, 1095–1102 (2009).

Watanabe, Y. Geometry and force behind kinetochore orientation: lessons from meiosis. *Nat Rev Mol Cell Biol* 13, 370-382 (2012).

Watanabe, Y. Modifying sister chromatid cohesion for meiosis. *J. Cell Sci.* 117, 4017-4023 (2004).

Yokobayashi, S. & Watanabe, Y. The kinetochore protein Moa1 enables cohesion-mediated monopolar attachment at meiosis I. *Cell* 123, 803-817 (2005).

Published paper

Kim J.*, Ishiguro K.*, Nambu A., Akiyoshi B., Yokobayashi S., Kagami A., Ishiguro T., Pendas A. M., Takeda N., Sakakibara Y., Kitajima T. S., Tanno Y., Sakuno T. and Watanabe Y.
(*equal contribution)
“ Meikin is a conserved regulator of meiosis I specific kinetochore function.”
Nature 517, 466-71 (2015).

Acknowledgements

This study was done during seven and half years in the Watanabe laboratory at the University of Tokyo IMCB (Institute of Molecular and Cellular Biosciences). I joined this project in the last five years as my PhD study, and it was my great pleasure.

I would like to express my sincere appreciation to my supervisor, Prof. Yoshinori Watanabe, for his excellent advice, caring, patience, passion and providing me with an excellent atmosphere for doing scientific research.

I would like to thank Dr. Ishiguro who was a collaborator in this study, and also let me experience the research of chromosome dynamics and practical experiments. Without his guidance, I could not have finished my PhD study. I would also like to thank Dr. Tanno, who as a good friend was always willing to help me and give his best suggestions. I would like to express my appreciation to Dr. Nambu, who found MEIKIN.

Many thanks to Dr. Morimoto, Dr. Shibuya and Yamamoto-kun as a mouse-team, and all past and present members of the Watanabe laboratory for their support and discussions. My special thanks to Oodan-san and Kasuya-san for their careful concern and favor. I would also like to thank Prof. Gotoh and all members of the Gotoh laboratory for discussion, mouse experimental guidance and friendship.

I would like to thank Dr. Kitajima and Dr. Sakakibara (RIKEN CDB) for their great work in oocyte live cell imaging and for discussion. I would also like to thank Dr. Takeda (Kumamoto Univ.) for generating the *Meikin* chimeric mice, and Dr. Yamazumi (Akiyama laboratory, IMCB) for his kind instruction in histological sample preparation. I would like to thank Dr. Pendás (CSIC–USAL, Spain) for *Sgo2 KO* mice and Dr. Tachibana-Konwalski (IMBA, Austria) for *Mlh1 KO* mice.

Finally, I am grateful to MEXT (Ministry of Education, Culture, Sports, Science and Technology, 文部科学省), the University of Tokyo and JSPS (Japan Society for the Promotion of Science, 日本学術振興会) for their financial support.

December, 2014

Jihye Kim

Figures and Legends

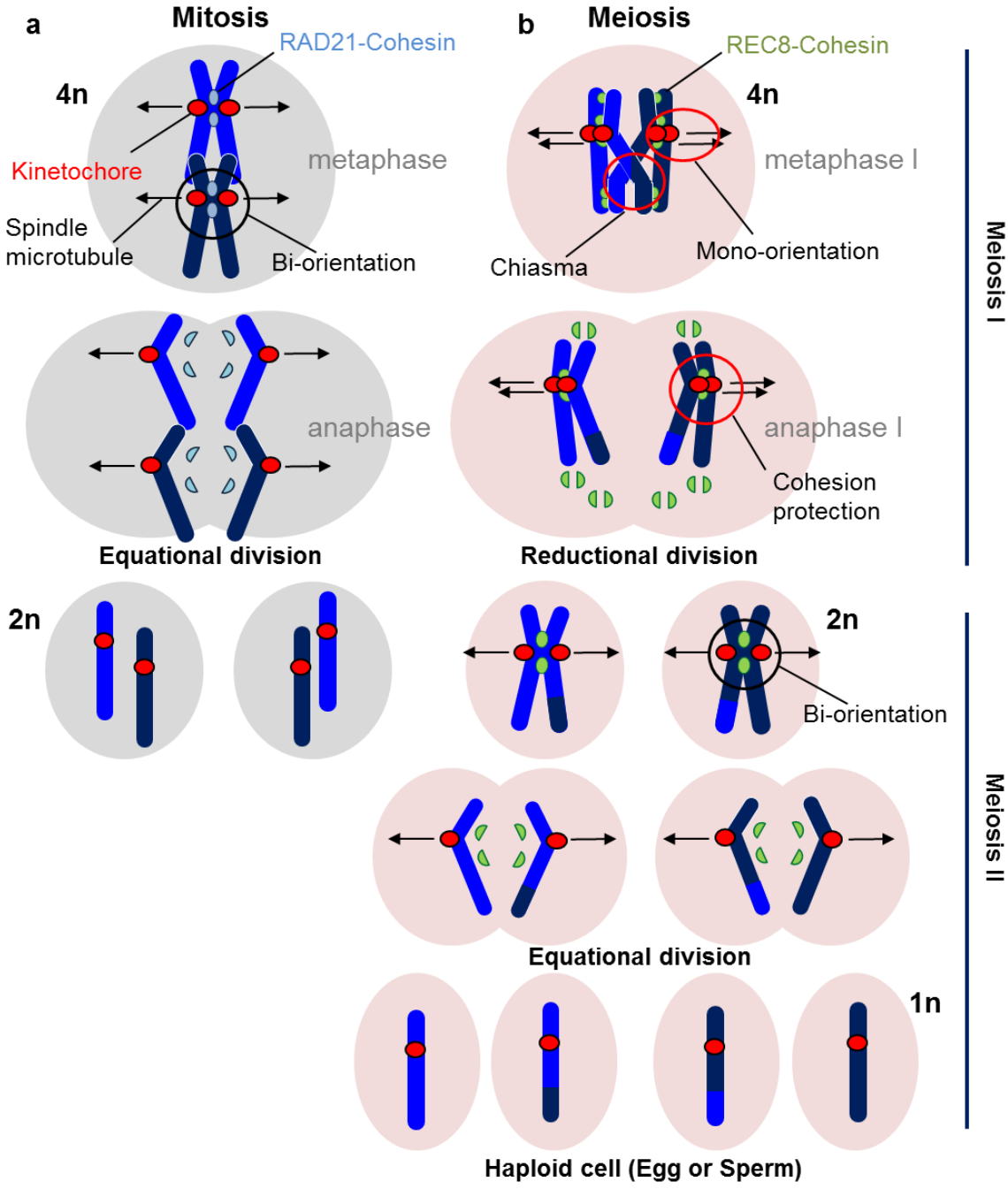

Figure 1. Chromosome segregation in mitosis and meiosis

Schematic drawing of behavior of chromosomes segregation during mitosis and meiosis. **a,** In mitosis, sister kinetochores are captured by spindle microtubules emanating from opposite poles. Sister chromatid cohesion mediated by Rad21-cohesin complexes is removed from the entire chromosomes at anaphase, allowing sister chromatid equational division into two daughter cells. **b,** In meiosis, Rad21 is largely replaced by meiosis-specific Rec8-cohesin complexes. During meiosis I, homologues are connected by chiasma and a pair of sister kinetochores is captured by spindle microtubules originating from a same spindle pole. Additionally, at the onset of anaphase I, centromeric cohesion is protected while cohesion is removed along chromosome arm. Thus, homologous chromosomes, rather than sister chromatids, are segregated toward opposite poles. During meiosis II, in contrast, sister chromatids separate as in mitosis. As a result, four haploid nuclei are generated by meiosis.

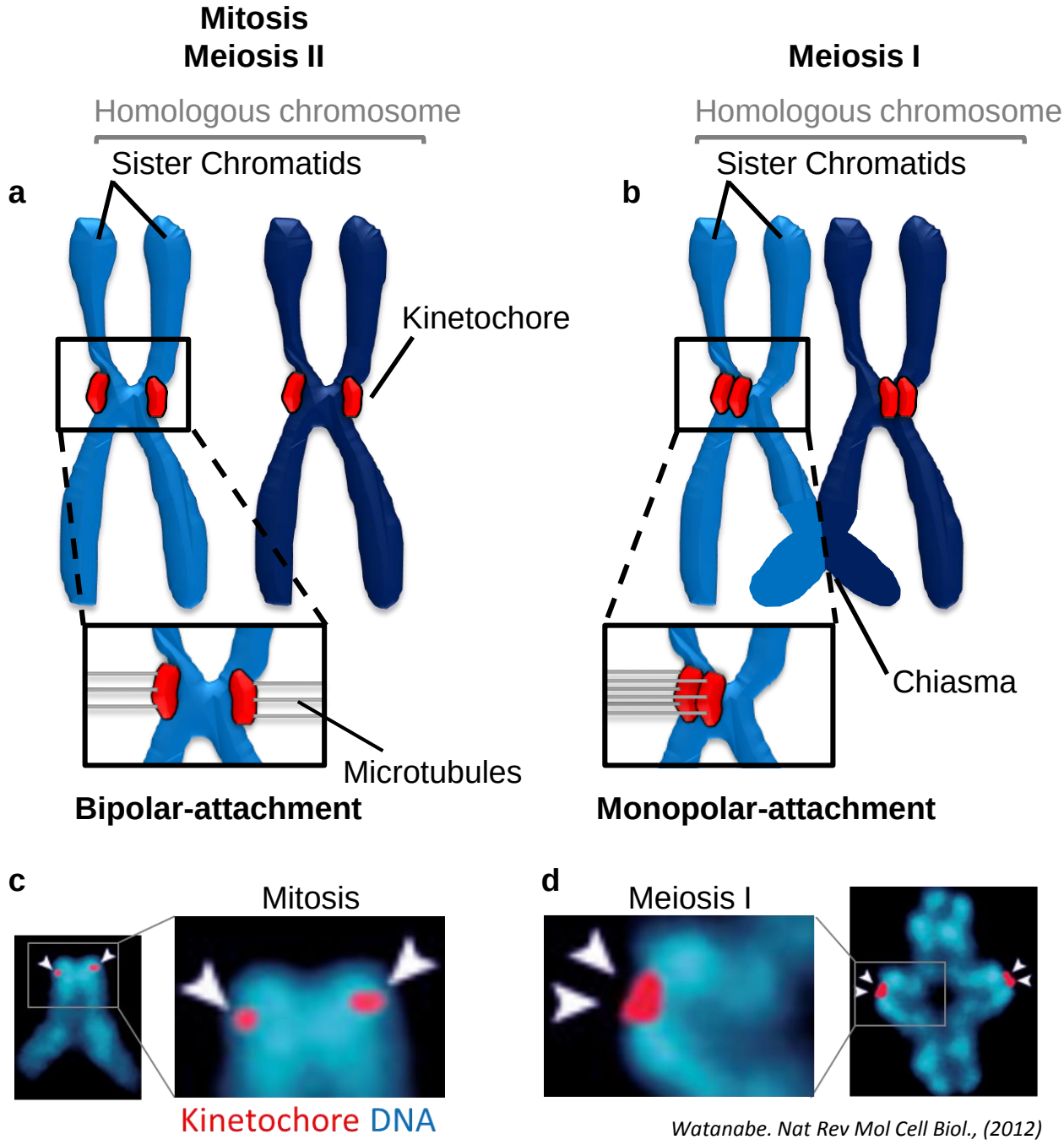

Figure 2. Sister kinetochore orientation during mitosis and meiosis

a, In mitosis (or meiosis II), sister kinetochores are separated and oriented back-to-back, therefore sister kinetochores are captured by spindle microtubules originating from opposite poles, known as bipolar-attachment. **b,** In meiosis I, homologous chromosomes are physically linked by chiasmata forming bivalents. Sister kinetochores are tightly fused and oriented side-by-side, thus are captured by microtubules from a same spindle pole, known as monopolar-attachment. **c,** The distinct kinetochore geometries of mitotic **d,** and meiotic (bivalent) chromosomes in mice. Centromere protein C (CENP-C) is labelled in red as a marker of kinetochore, and chromosomes are shown in blue, two white arrow heads mark a pair of sister kinetochore.

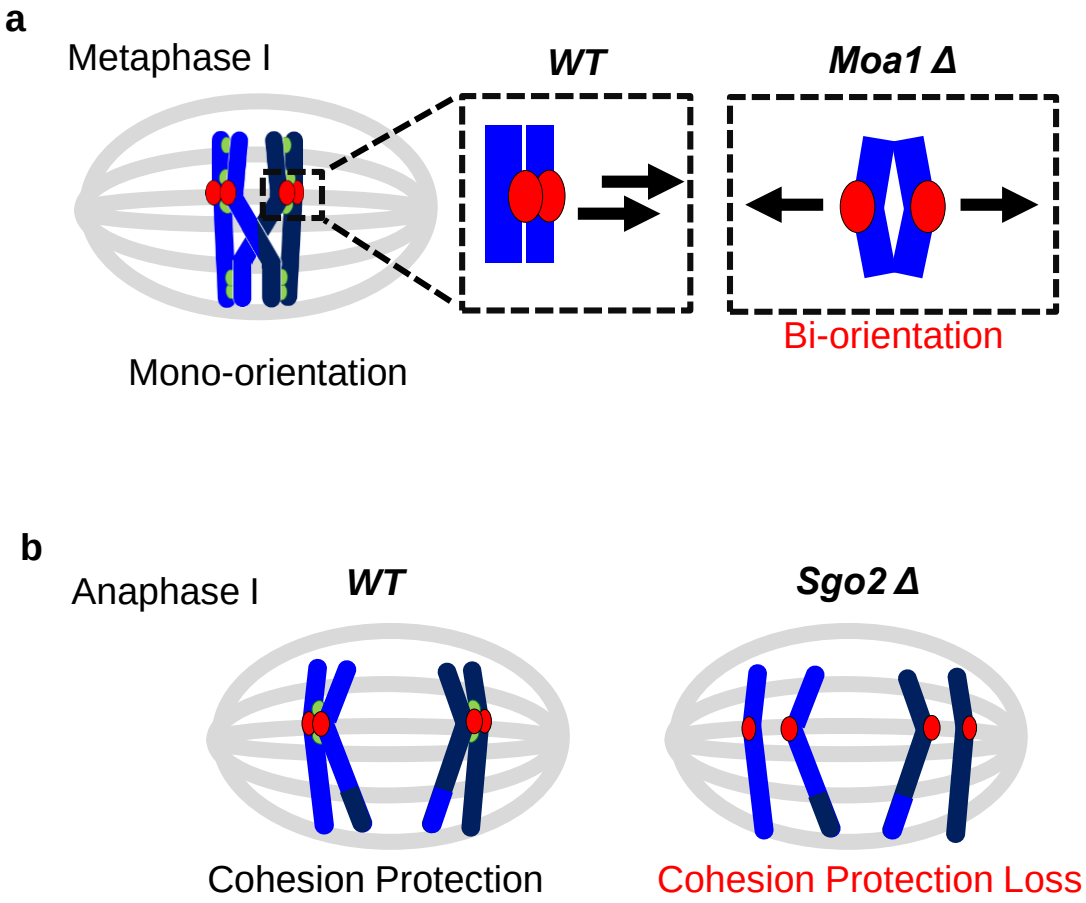

Figure 3. Unique Meiosis I Kinetochore Regulation
a, Moa1, meiosis I specific kinetochore protein in fission yeast, regulates mono-orientation during meiosis I.
b, Conserved centromeric protein shugoshin (SGO2) protects centromeric cohesion during anaphase I.

a

Isolated clones	frequency
4930404A10Rik	42
Thap7	15
Zfp438	12
BC051142	12
4930519N13Rik	3
Htatip	1
Nsun7	1
Scrib	1
Tuft1	1
Spesp1	1
Snf1lk	1
Acbd3	1
Ncor1	1
Total	92

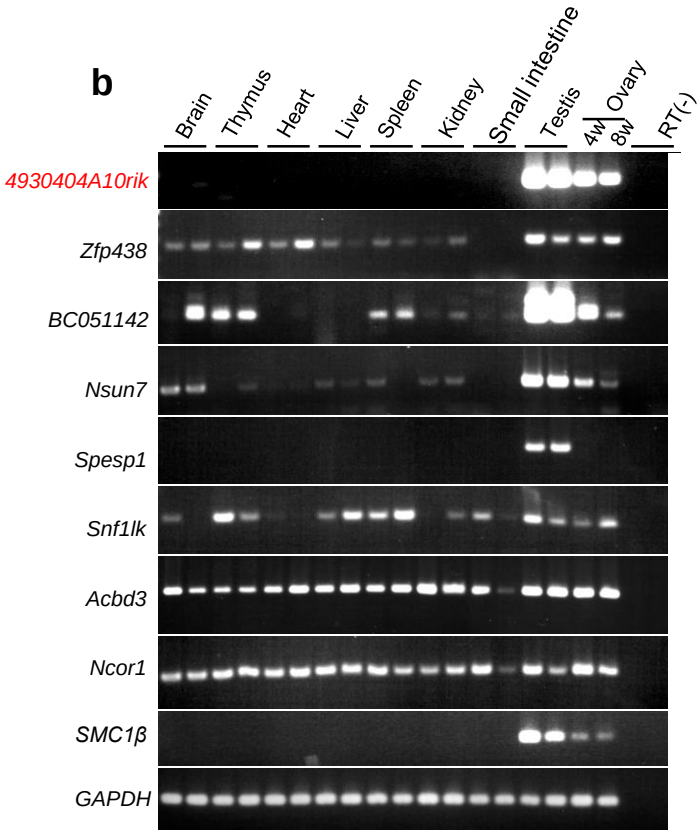

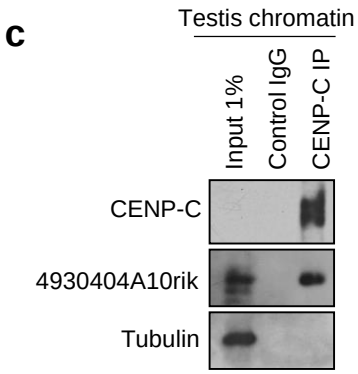

Figure 4. CENP-C interacting novel protein, 4930404A10rik

a, Yeast two hybrid screening using mCENP-C C-terminus (a.a. 692-906) as bait from mouse testis cDNA library. 11.95 x10^7 colonies were screened on the selective (SD-Trp-Leu-His-Ade, +10mM 3AT) plates. The number of clones isolated by screening is summarized. **b,** RNA was extracted from each tissue of both male and female. Testis were derived from different 8-week males. ovary RNA were derived from 4- and 8-week animals. RT(-) indicates control PCR in the presence of testis RNA without reverse transcription. **c,** Immunoprecipitates from mouse testis chromatin extracts using anti-CENP-C antibody or control IgG were analyzed by the indicated antibody. **(Note, `a` was performed by Dr. Nambu and `b-c` were performed by Dr. Ishiguro.)**

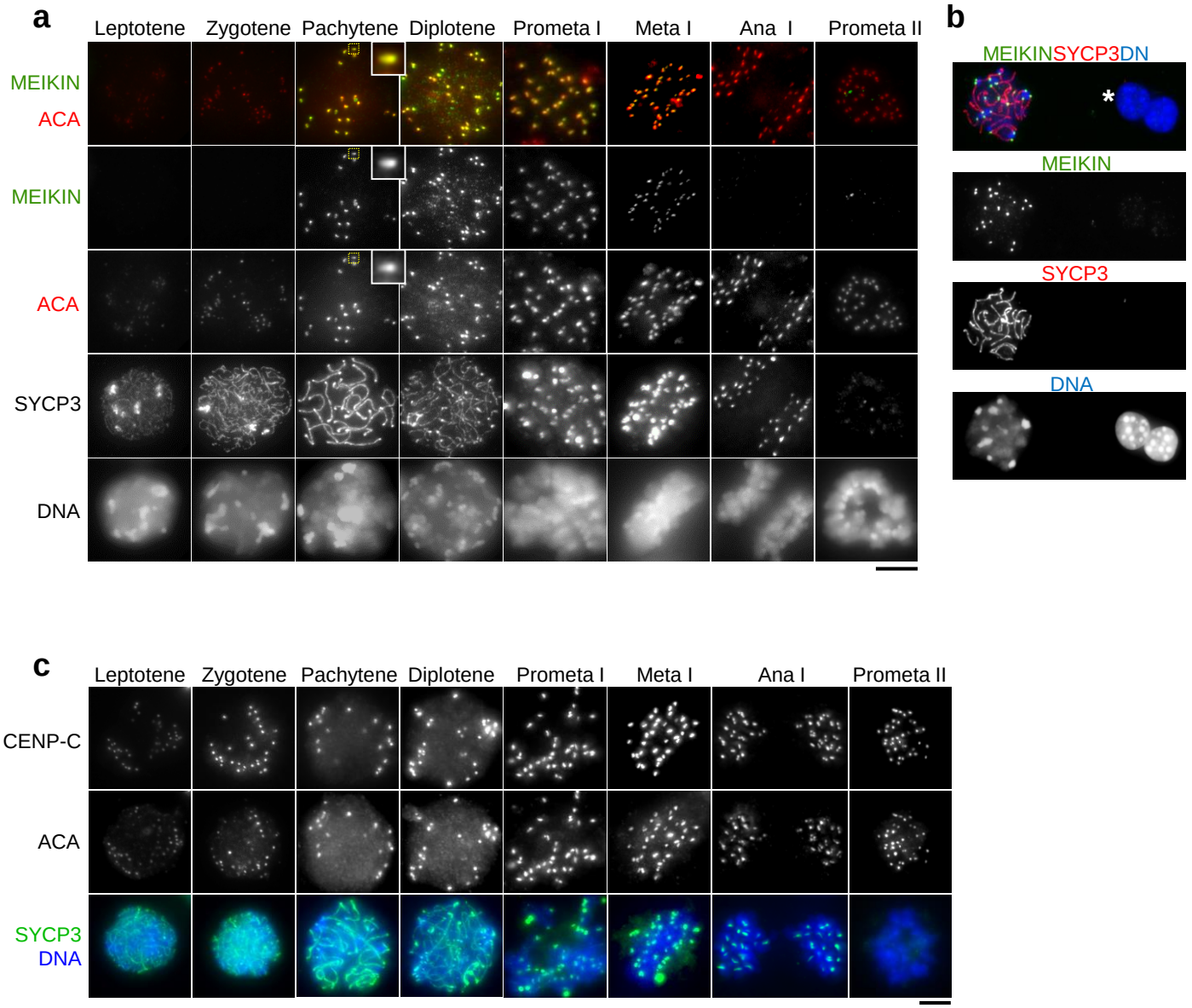

Figure 5. MEIKIN (*4930404A10rik*) localizes to kinetochore in meiosis I.
a, Squashed spermatocytes from wild-type were stained for MEIKIN, ACA, SYCP3 and DAPI (DNA); prometaphase I (Prometa I), metaphase I (meta I) and prometaphase II (Prometa II). **b,** a spermatocyte (pachytene) and two spermatogonia cells (mitotic cells, marked by asterisk) from wild-type were stained for MEIKIN, SYCP3 and DAPI (DNA) **c,** Squashed spermatocytes from wild-type were immunostained for CENP-C, ACA, SYCP3 and DAPI at the indicated stages during meiosis. CENP-C and ACA signals accumulate and colocalize at centromeres after zygotene throughout meiosis.

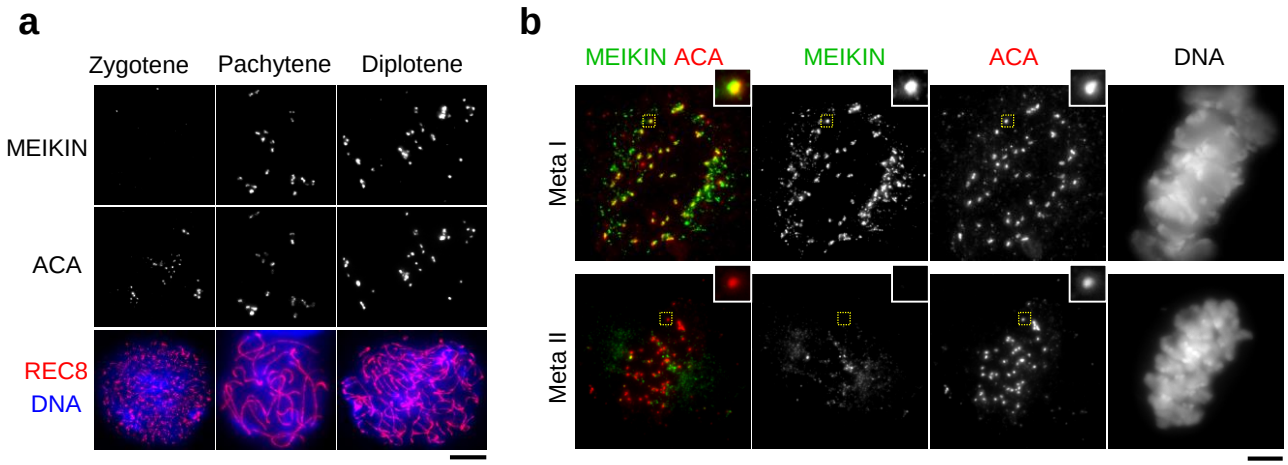

Figure 6. MEKIN localization in oocytes.
a, Chromosome spreads of oocytes from wild-type were immunostained for MEIKIN, ACA and REC8 at different meiotic stages. Zygotene from E15.5, Pachytene and Diplotene from E18.5 mouse. **b,** Chromosome spreads of oocytes at metaphase I (5 h post GVBD) and metaphase II (16 h post GVBD) were stained for MEIKIN, ACA and DAPI. Scale bars, 5 μm.

Figure 7. Sequence alignment of MEIKIN homologs in vertebrates.
Amino acid sequences of *M. musculus* 4930404A10Rik (NP_083381), *R. norvegicus* (XP_573090), *C. lupus* (XP_003639413), *X. tropicalis* (XP_002934413) and *G. gallus* (XP_001234011) were derived from the NCBI protein database. *H. sapiens* data was derived from our own sequencing of cDNA clones. The 4930404A10Rik protein is conserved among vertebrates but it does not have any other known motif except the polo-box binding motif (blue line) present in mammalian proteins. Two-hybrid assays indicate that this motif in mouse MEIKIN is important for PLK1 binding (data not shown), although the motif is apparently not conserved in Xenopus and chicken. The C-terminal sequences (red lines) are required for kinetochore localization (see Fig. 8c-d). **(Note, Alignment was performed by Dr. Ishiguro)**

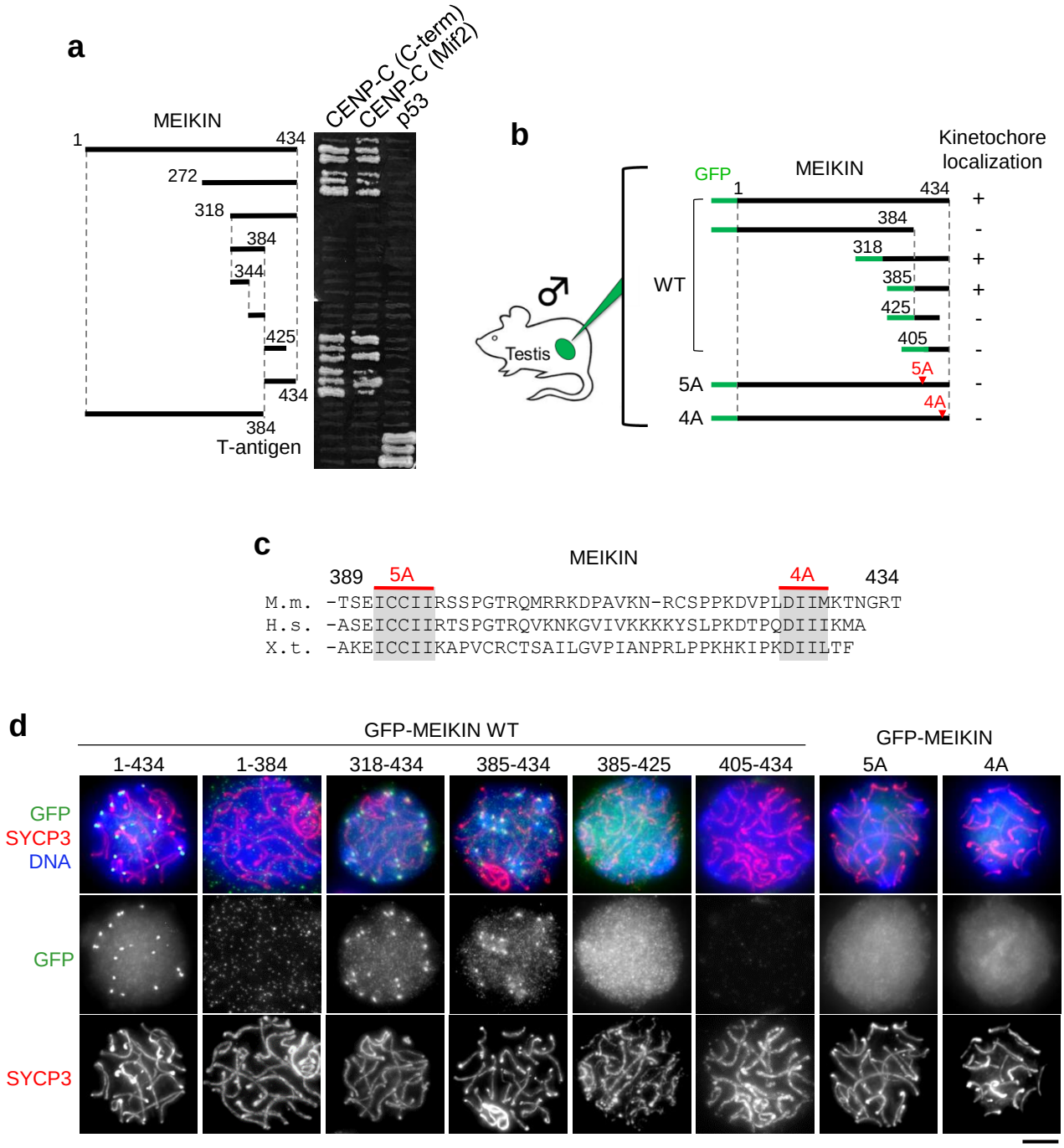

Figure 8. MEIKIN C-terminus is important to interact with CENP-C

a, The C-terminal domain of 4930404A10rik (a.a. 385-434) interacts with the CENP-C C-terminus (692-906 aa.) or CENP-C mif2 motif (801-906 aa.) in yeast two-hybrid assay. **b,** Schematic illustrations of GFP-tagged MEIKIN fragments and mutants with the summary of their kinetochore localization: localized (+) or not localized (-). **C,** Alanine substitutions (5A and 4A, marked by gray shade and red lines) were introduced on the C-terminal conserved sequences of MEIKIN (also see Fig. 7). **d,** Spermatocytes from the wild-type testis transfected with GFP-tagged MEIKIN stained for GFP, SYCP3 and DAPI (DNA).

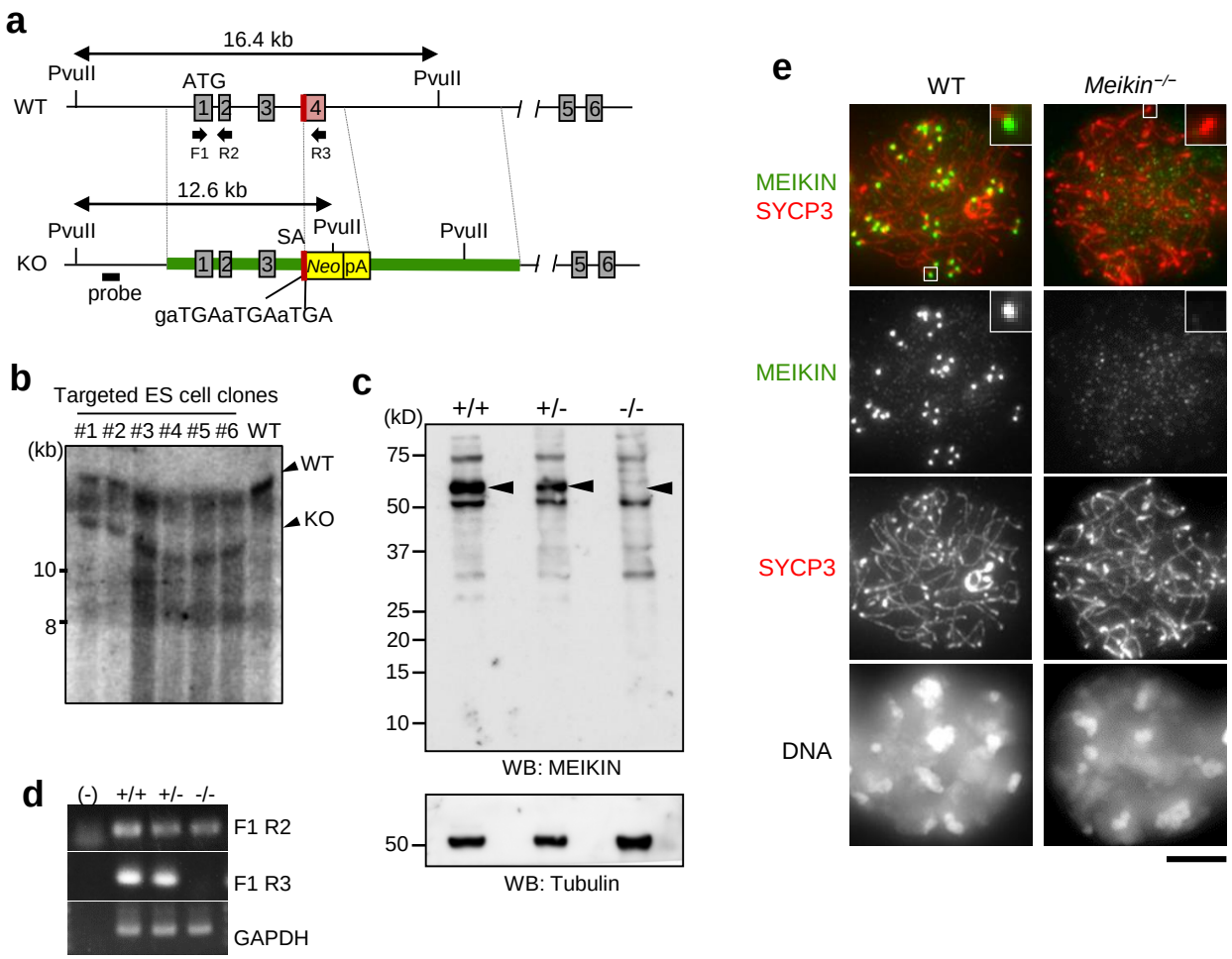

Figure 9. Generation of *Meikin*-knockout mice.
a, Schematic illustrations of the wild-type allele and targeted *Meikin*$^{-/-}$ allele are shown. Grey boxes represent exons. The targeted exon 4 contains the intact splicing acceptor (SA) sequence followed by a premature stop codon, resulting in disruption of the *Meikin* allele. Black arrows, primers for RT-PCR. **b,** Southern blot of genomic DNA from wild type (+/+) and *Meikin* heterozygous (+/-) ES cells after Pvu II digestion. ES cell clone #2 used to generate the mice. **c,** Western blotting analysis of testis extracts prepared from mice with the indicated genotypes (4-week-old). In *Meikin*$^{-/-}$, the specific bands probed by the anti-MEIKIN antibody are absent (marked by black arrowheads). α-tubulin is a loading control. **d,** RT-PCR analysis of mRNA purified from mouse testis with the indicated genotypes. **e,** The diplotene spermatocytes from wild-type (+/+) and *Meikin*$^{-/-}$ (-/-) were immunostained for MEIKIN and SYCP3. Enlarged images of a kinetochore are shown. **e,** WT and *Meikin*$^{-/-}$ round spermatids stained for CENP-C and DAPI (DNA). ****$P < 0.0001$, unpaired *t*-test. Scale bar, 5 μm. **(Note that `a` targeting vector was designed by Dr. Ishiguro)**

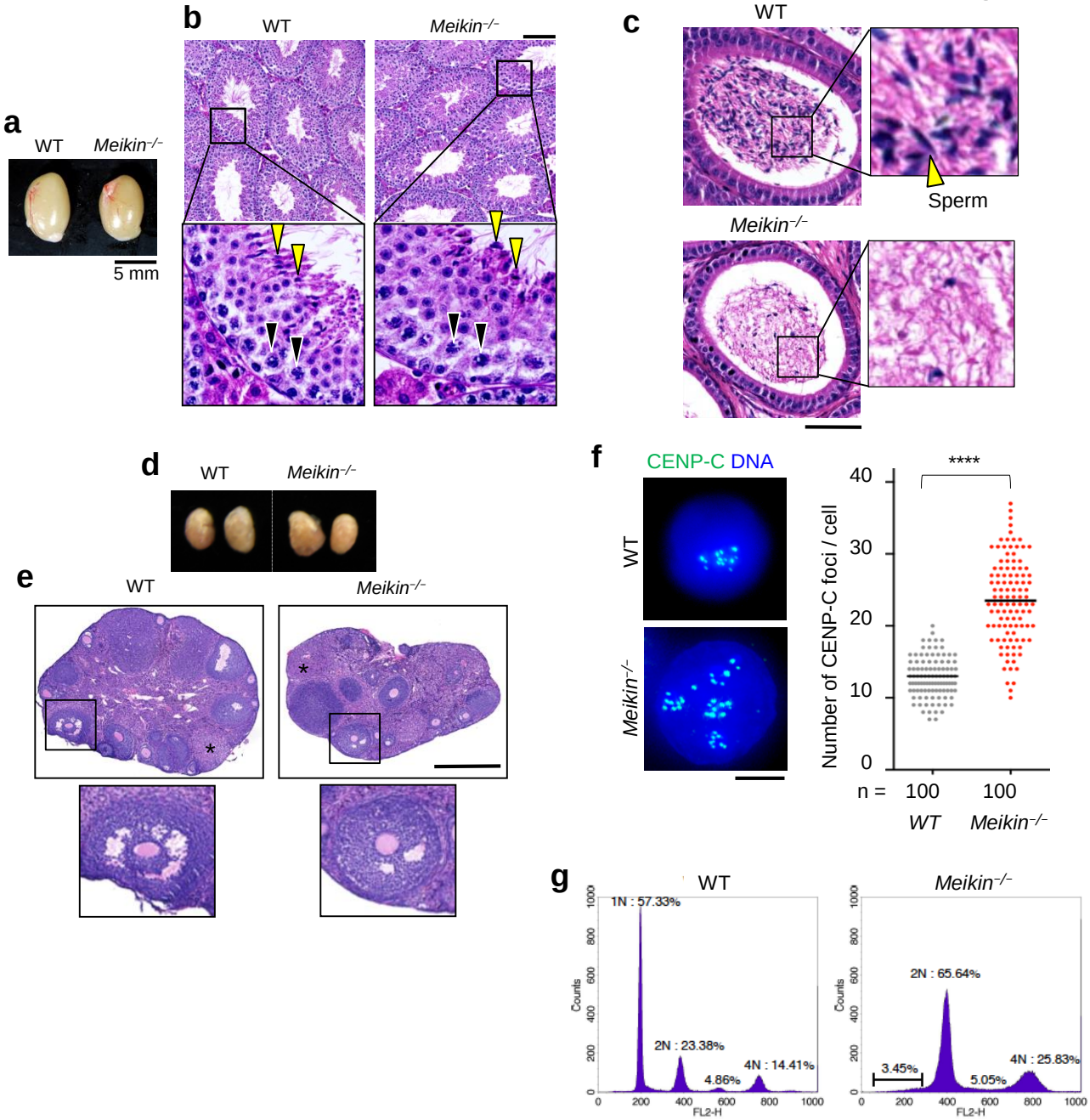

Figure 10. *Meikin* KO is infertile

a, Testes from 12 week-old wild-type and *Meikin*$^{-/-}$ mice. **b,** Hematoxylin-eosin staining of a section of the testis (12-week-old) showed seminiferous tubules. Enlarged pictures of seminiferous tubules showed spermatocytes (black arrowheads) and spermatids (yellow arrowheads) in wild-type and *Meikin*$^{-/-}$. Scale bar, 100 μm. **c,** Hematoxylin-eosin staining of epididymis from 12-week-old mice shows reduced number of sperms in *Meikin*$^{-/-}$. Enlarged images of sperms are shown. Scale bar, 50 μm **d,** A pair of ovaries (8-week-old) from the indicated genotypes (top). **e,** Hematoxylin and eosin–stained paraffin sections of ovaries from 8-week-old wild-type and *Meikin*$^{-/-}$ mice (middle). The antral-stage follicles with oocyte nuclei are magnified (bottom). Asterisks indicate corpora lutea. Scale bar, 500 μm. **f,** WT and *Meikin*$^{-/-}$ round spermatids stained for CENP-C and DAPI (left). The number of CENP-C foci per cell is represented in a scatter plot with median (n = cell number) (right). ****$P < 0.0001$, unpaired *t*-test. **g,** Cell population in a testis was examined by FACS in wild-type and *Meikin*$^{-/-}$ (8-week old). Scale bar, 5 μm **(Note, `g` was performed by Dr. Ishiguro)**

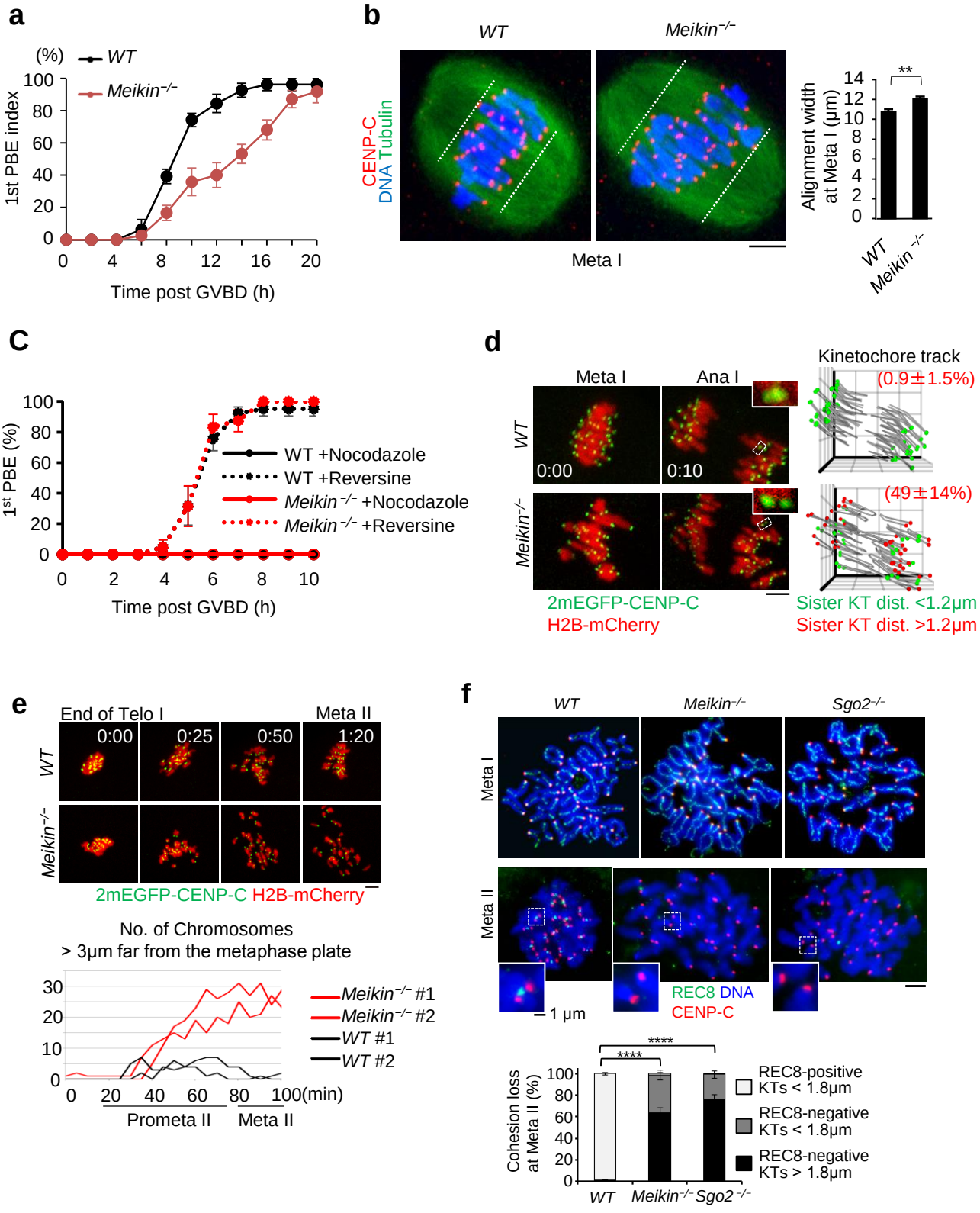
a
(%)
WT
Meikin−/−
1st PBE index
Time post GVBD (h)
b
WT
Meikin−/−
CENP-C
DNA Tubulin
Meta I
Alignment width at Meta I (μm)
**
C
1st PBE (%)
WT +Nocodazole
WT +Reversine
Meikin −/− +Nocodazole
Meikin −/− +Reversine
Time post GVBD (h)
d
Meta I
Ana I
Kinetochore track
(0.9±1.5%)
(49±14%)
0:00
0:10
2mEGFP-CENP-C
H2B-mCherry
Sister KT dist. <1.2μm
Sister KT dist. >1.2μm
e
End of Telo I
Meta II
0:00
0:25
0:50
1:20
2mEGFP-CENP-C H2B-mCherry
No. of Chromosomes
> 3μm far from the metaphase plate
Meikin−/− #1
Meikin−/− #2
WT #1
WT #2
Prometa II
Meta II
f
Meta I
Meta II
REC8 DNA
CENP-C
1 μm
Cohesion loss at Meta II (%)
REC8-positive KTs < 1.8μm
REC8-negative KTs < 1.8μm
REC8-negative KTs > 1.8μm

Figure 11 (continue)

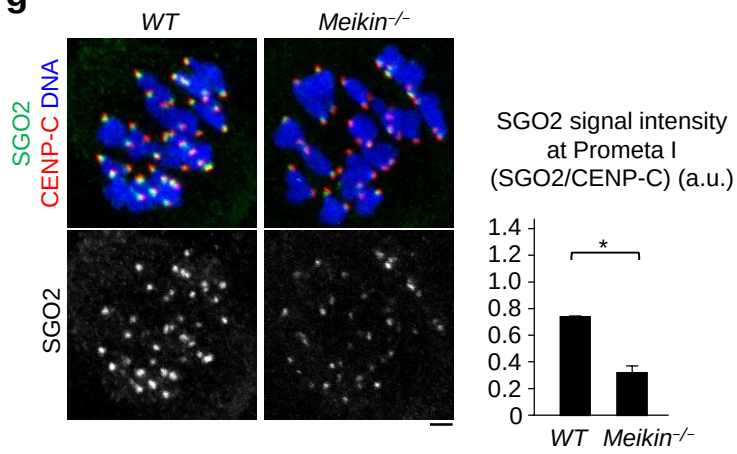

Figure 11. MEIKIN is required for the protection of centromeric cohesin during meiosis I.
a, Wild-type and *Meikin*$^{-/-}$ oocytes were cultured to undergo GVBD and meiosis I progression. Cumulative 1st polar body (1st PB) extrusion ratio after GV breakdown (GVBD, t = 0) are shown with mean ± s.e.m. from 4 independent experiments. Total number of oocytes was 40 for wild-type (7, 12, 8 and 13, respectively), 58 for *Meikin*$^{-/-}$ (12, 22, 14 and 10, respectively). **b,** Oocytes in metaphase I (Meta I, 6 h post GVBD) were stained for α-tubulin, CENP-C and DAPI (left). The chromosome alignment widths (the distance between distal kinetochores indicated by white dashed lines) were measured (right). Error bars, s.e.m. from 3 independent experiments. 10 oocytes were counted in each experiment. **c,** Oocytes from wild-type and *Meikin*$^{-/-}$ mice were cultured after GVBD in the presence of nocodazol (10 μM) or the Mps1 kinase inhibitor reversin (5μM). The first polar body extrusion (PBE) rates are shown with mean ± s.e.m. from 3 independent experiments. Total number of oocytes is 27 in WT with nocodazole (7, 10 and 10, respectively), 27 for WT with reversine (6, 10 and 11. respectively), 21 for *Meikin*$^{-/-}$ with nocodazol (5, 8 and 8, respectively) and 23 for *Meikin*$^{-/-}$ with reversine (7, 8 and 8, respectively). **d,** Time-lapse imaging of the first meiotic division in oocytes expressing 2mEGFP-CENP-C and H2B-mCherry. The maximum intensity z-projection images at metaphase I (Meta I) and anaphase I (Ana I) are shown (left). Time after Meta I (h:mm) is marked on the figures. The images were reconstructed in 3D, and kinetochore tracks are indicated by grey lines (right). The sister kinetochore distances at anaphase I are color-coded as indicated. The ratios of separated sister kinetochores (distance > 1.2 μm) at anaphase I were measured in 3 oocytes (mean ± s.d.). **e,** Time-lapse imaging of the second meiotic division in oocytes as in **c** (upper). Resumption of kinetochore movement after 1st PBE was assumed as the end of telophase I (Telo I). Time after the end of Telo I (h:mm) is marked on the figures. The number of kinetochores with distance > 3 μm from the metaphase plate were counted over time and shown in the graph (bottom). **f,** Chromosome spreads of oocytes at metaphase I (Meta I, 7.5 h post GVBD) and metaphase II (Meta II, 20 h post GVBD) were stained for REC8, CENP-C and DAPI (upper). The spread chromosomes at metaphase II were classified into three categories according to REC8 signals and kinetochore distance, each of which is shown in the graph (bottom) with mean ± s.e.m. from 3 independent experiments. 5 oocytes were counted in each experiment. *P*-values indicate the outcome of unpaired *t*-test from REC8-negative categories. **g,** Oocytes in prometaphase I (4 h post GVBD) were stained for SGO2, CENP-C and DAPI in whole mount (left). The signal intensity of SGO2 adjacent to the centromere was quantified and normalized to that of CENP-C. The relative intensities are shown with mean + s.e.m. from 3 independent experiments (right). In each experiment, 15 centromeres from an oocyte were quantified (n = 5 cells). *P < 0.05, **P < 0.01, ****P < 0.0001, unpaired *t*-test (**b, f, g**). Scale bars, 5 μm. **(Note, `d and e` were performed by Dr. Kitajima and Dr. Sakakibara.)**

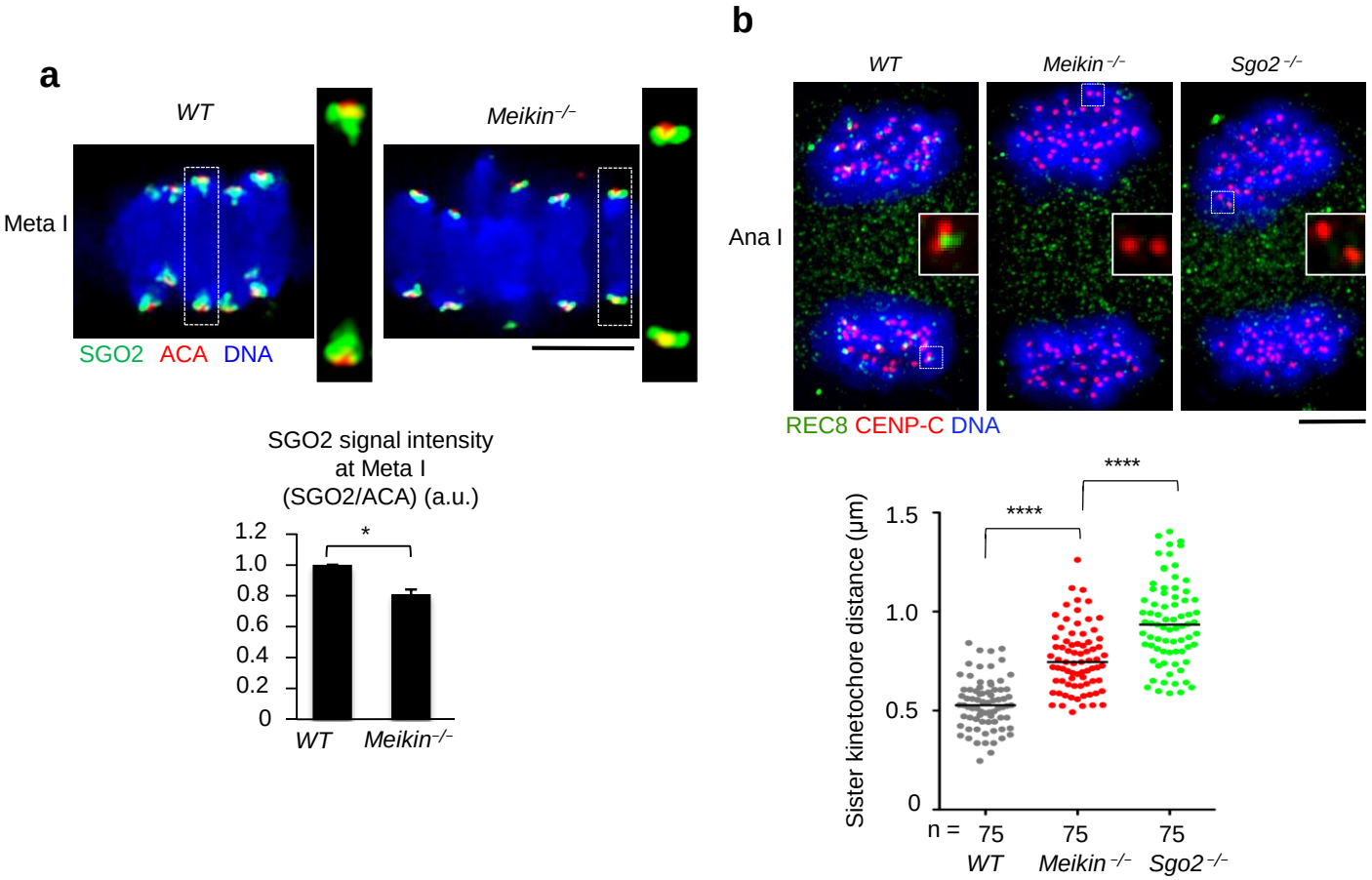

Figure 12. MEIKIN is required for centromeric cohesion protection in spermatocytes.
a, Squashed spermatocytes at metaphase I (Meta I) were immunostained for SGO2, ACA and DAPI. Partial z-projection images of aligned chromosomes are shown with magnified images of a bivalent (upper). The signal intensity of SGO2 adjacent to the centromere was quantified and normalized to that of ACA. The relative intensities are shown with mean + s.e.m. from 3 independent experiments (bottom). In each experiment, 15 centromeres from a spermatocyte were quantified (n = 5 cells). **b,** Squashed spermatocytes at anaphase I (5 μm < segregated DNA mass distance < 10 μm) from wild-type, *Meikin*$^{-/-}$ and *Sgo2*$^{-/-}$ mice were immunostained for CENP-C, REC8 and DNA (upper). A pair of sister kinetochores is magnified. The distance of sister kinetochores was scored and represented in the scatter plot with median (bottom). 15 kinetochores from 5 spermatocytes were measured in each group (n = the number of sister kinetochores). * $P < 0.05$, **** $P < 0.0001$, unpaired *t*-test (**a,b**). Scale bars, 5 μm

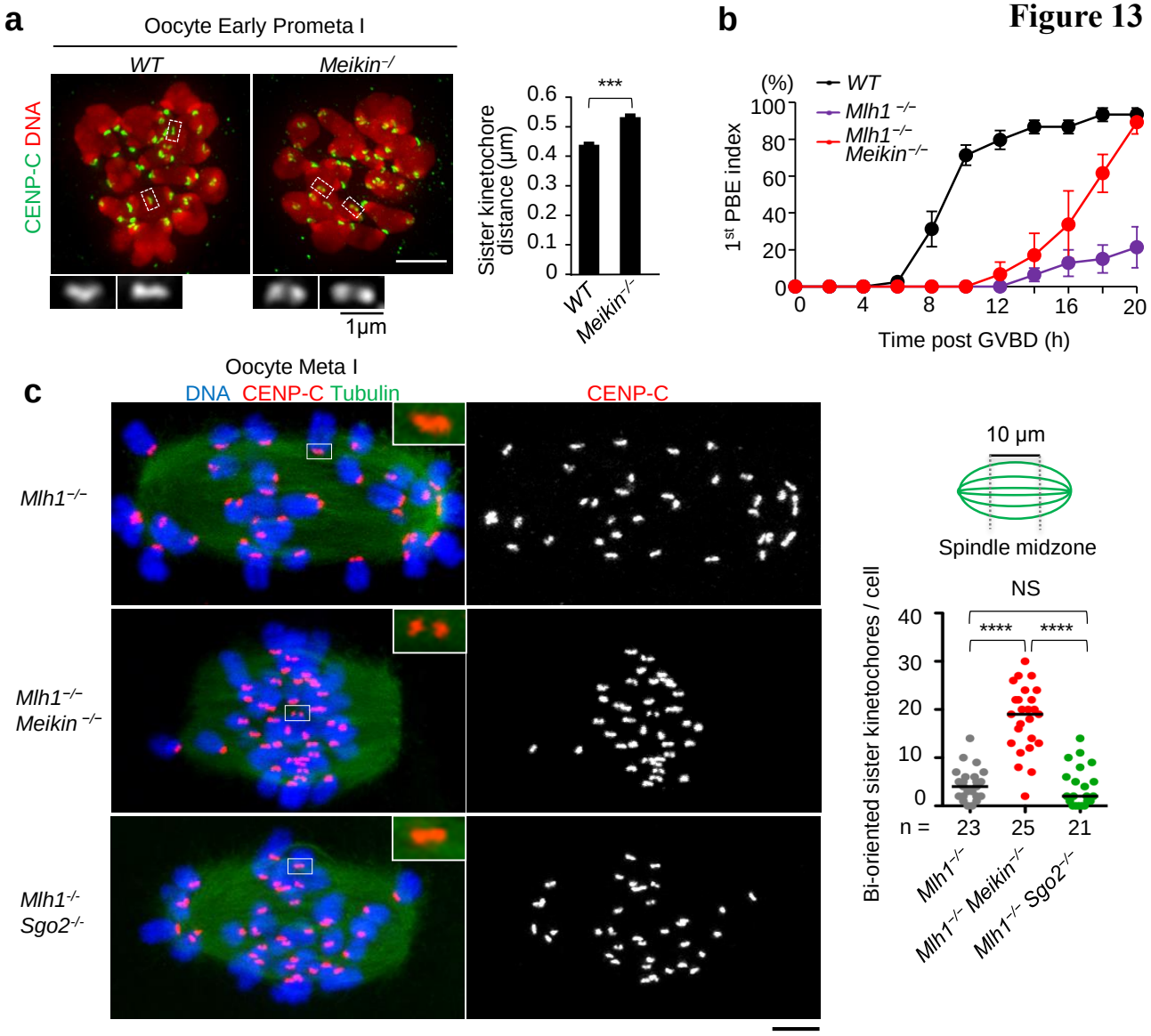

Figure 13. MEIKIN regulates mono-orientation in oocyte

a, Wild-type and *Meikin*$^{-/-}$ oocytes at early prometaphase I (2 h post GVBD) were stained for CENP-C and DAPI (left). The pairs of sister kinetochores are magnified. The distance between two CENP-C signals of a sister kinetochore pair on different z-planes was measured as sister kinetochore distance and represented in the graph with mean + s.e.m. from three independent experiments (right). In each experiment, 10 kinetochores were measured in a cell (n = 5 cells). **b,** Wild-type, *Mlh1*$^{-/-}$ and *Mlh1*$^{-/-}$ *Meikin*$^{-/-}$ oocytes were cultured to undergo GVBD and meiosis I progression. Cumulative 1st polar body (1st PB) extrusion ratio after GVBD (t = 0) are shown with mean ± s.e.m. from 3 independent experiments. Total oocyte number was 45 for wild-type (27, 8 and 10, respectively), 29 for *Mlh1*$^{-/-}$ (8, 15 and 6, respectively) and 29 for *Mlh1*$^{-/-}$ *Meikin*$^{-/-}$ (10, 10 and 9, respectively). **c,** Metaphase I oocytes (at 10 h post GVBD) stained for α-tubulin, CENP-C and DAPI in whole mount (left). Magnified images are shown to highlight bi-oriented sister kinetochores at the spindle midzone in *Mlh1*$^{-/-}$ and *Mlh1*$^{-/-}$ *Meikin*$^{-/-}$. The number of bi-oriented sister kinetochores at the spindle midzone (10 μm width centered between spindle poles; only spindles up to 30 μm in length were used) was scored and represented in the scatter plot with the median from three independent experiments (n = cell number) (right). Bi-oriented sister kinetochores were determined by sister kinetochore distance > 0.6 μm with horizontal angle (0-10˚). The sister kinetochore distance was measured as the distance between two highest peak CENP-C signals. NS, not significantly different. Note that *Mlh1*$^{-/-}$ *Meikin*$^{-/-}$ was compared to *Mlh1*$^{-/-}$ with C57BL/6 background littermates. *** $P < 0.001$, ****$P < 0.0001$, unpaired *t*-test (**a-c**). Scale bars, 5 μm (unless otherwise indicated).

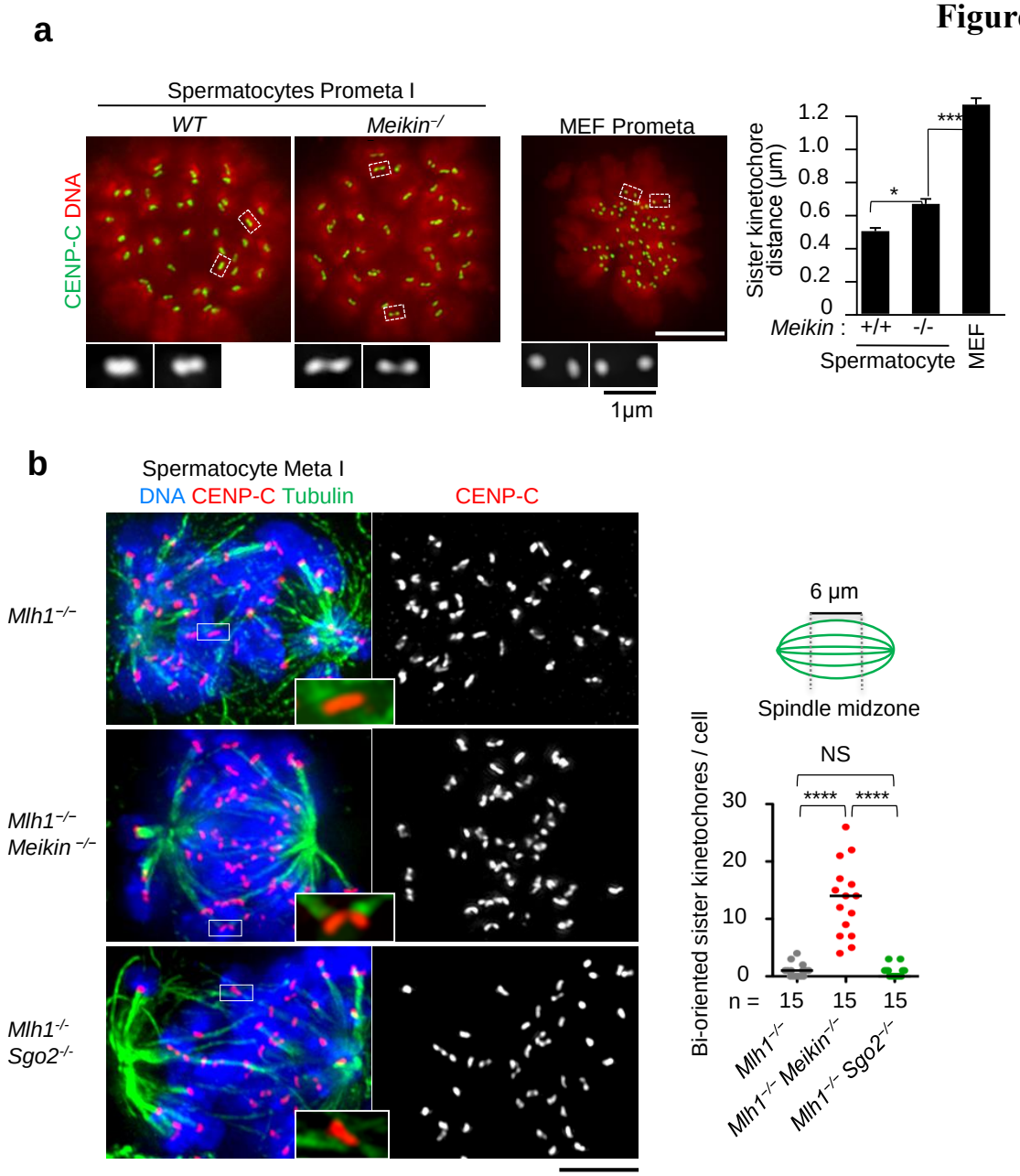

Figure 14. MEIKIN regulates mono-orientation in spermatocyte

a, Squashed spermatocytes at prometaphase I from wild-type and *Meikin*$^{-/-}$ mice, and MEF cells at prometaphase (prometa) were immunostained for CENP-C and DNA. Pairs of sister kinetochores are magnified. The distances between sister kinetochores were scored and represented in the graph with mean + s.e.m. from three independent experiments (right). Note that, MEF cells sample preparation and sister kinetochore distance measurements were performed same methods with spermatocytes. In each experiment, 10 kinetochores were measured in a cell (n = 5 cells). **b,** Squashed spermatocytes at metaphase I were stained for α-tubulin, CENP-C and DAPI (left), and the number of bi-oriented sister kinetochores was scored and represented in the scatter plot with the median from two independent experiments (n = cell number) (right) as in Fig.13**c** (n = cell number). Spindle midzone, 6 μm (only spindles up to 15 μm in length were used). Sister kinetochores distance > 0.6 μm as 'bi-oriented'. NS, not significantly different. Note that *Mlh1*$^{-/-}$ *Meikin*$^{-/-}$ was compared to *Mlh1*$^{-/-}$ with C57BL/6 background littermates. *** $P < 0.001$, ****$P < 0.0001$, unpaired *t*-test (**a, b**). Scale bars, 5 μm (unless otherwise indicated).

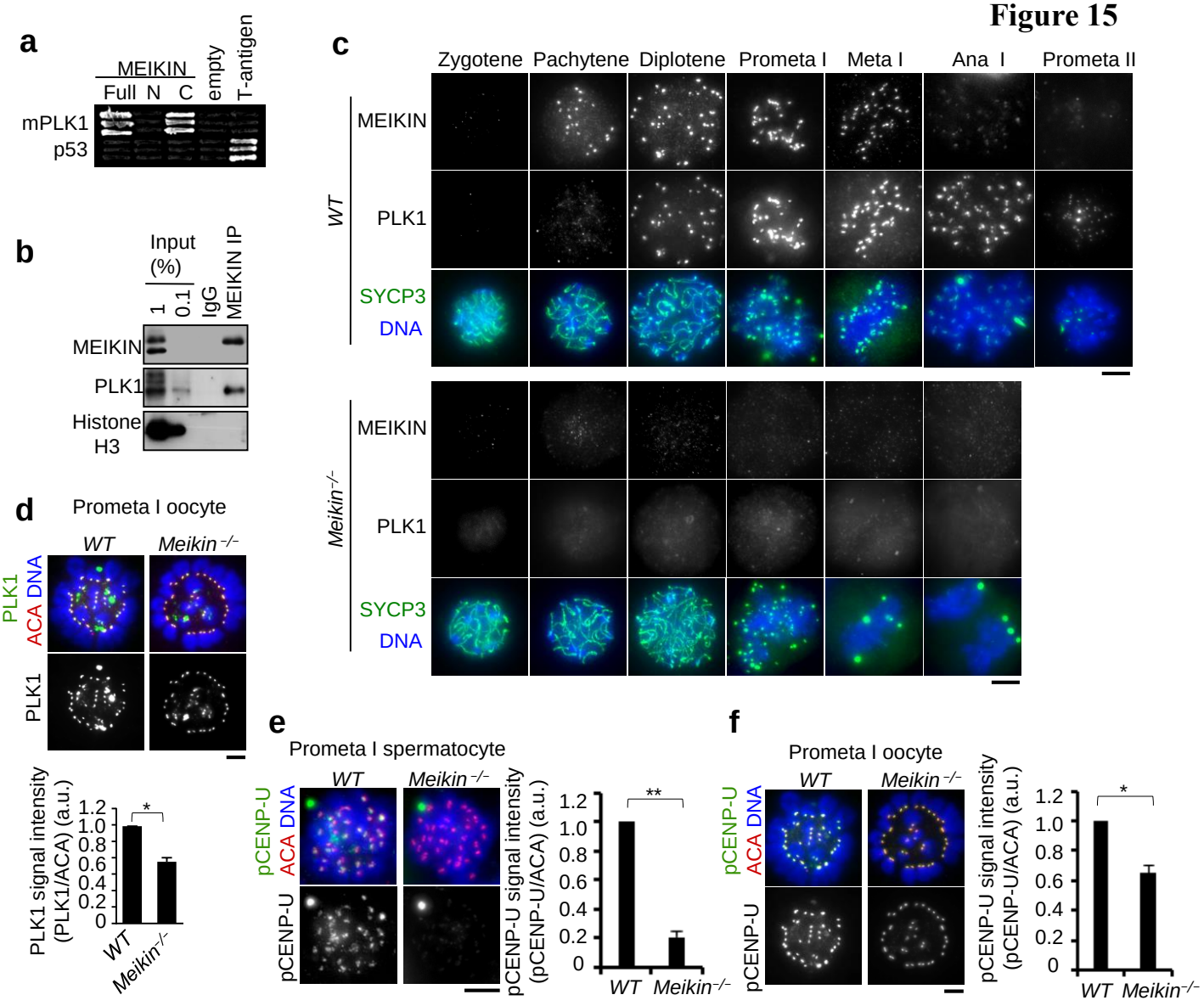

Figure 15. MEIKIN dependent PLK1 accumulates to kinetochore during meiosis I

a, Yeast two hybrid assay demonstrates that MEIKIN interacts directly with mouse PLK1 through the MEIKIN C-terminal domain (a.a. 272-434). **b,** Immunoprecipitates from mouse testis chromatin extracts using anti-MEIKIN antibody or control IgG were analyzed by the indicated antibody. PLK1 was co-immunoprecipitated with MEIKIN. **c,** Squashed spermatocytes from wild-type and *Meikin*$^{-/-}$ mice were immunostained for MEIKIN, PLK1, SYCP3 and DAPI at different meiotic stages. **d,** Chromosome spreads of oocytes at prometaphase I (3 h post GVBD) were stained for PLK1, ACA and DAPI (left). The relative intensities of PLK1 normalized to that of ACA are shown with mean + s.e.m. from 3 independent experiments (right). In each experiment, 15 kinetochores from each oocyte were quantified (n = 4 cells). **e,** Squashed spermatocytes at prometaphase I were stained for pCENP-U, ACA and DAPI (upper) The relative intensities of pCENP-U was normalized to that of ACA are shown with mean + s.e.m. from 3 independent experiments. In each experiment, 10 kinetochores from a spermatocyte were quantified (n = 5 cells). **f,** Chromosome spreads of oocytes at prometaphase I (3 h post GVBD) were stained for pCENP-U, ACA and DAPI (upper) The relative intensities of pCENP-U was normalized to that of ACA are shown with mean + s.e.m. from 3 independent experiments. In each experiment, 10 kinetochores from a oocyte were quantified (n = 4 cells). *p < 0.05, **p < 0.01, unpaired t-test (**d,e,f**) Scale bars, 5 μm. **(Note, `a and b` were performed by Dr. Ishiguro.)**

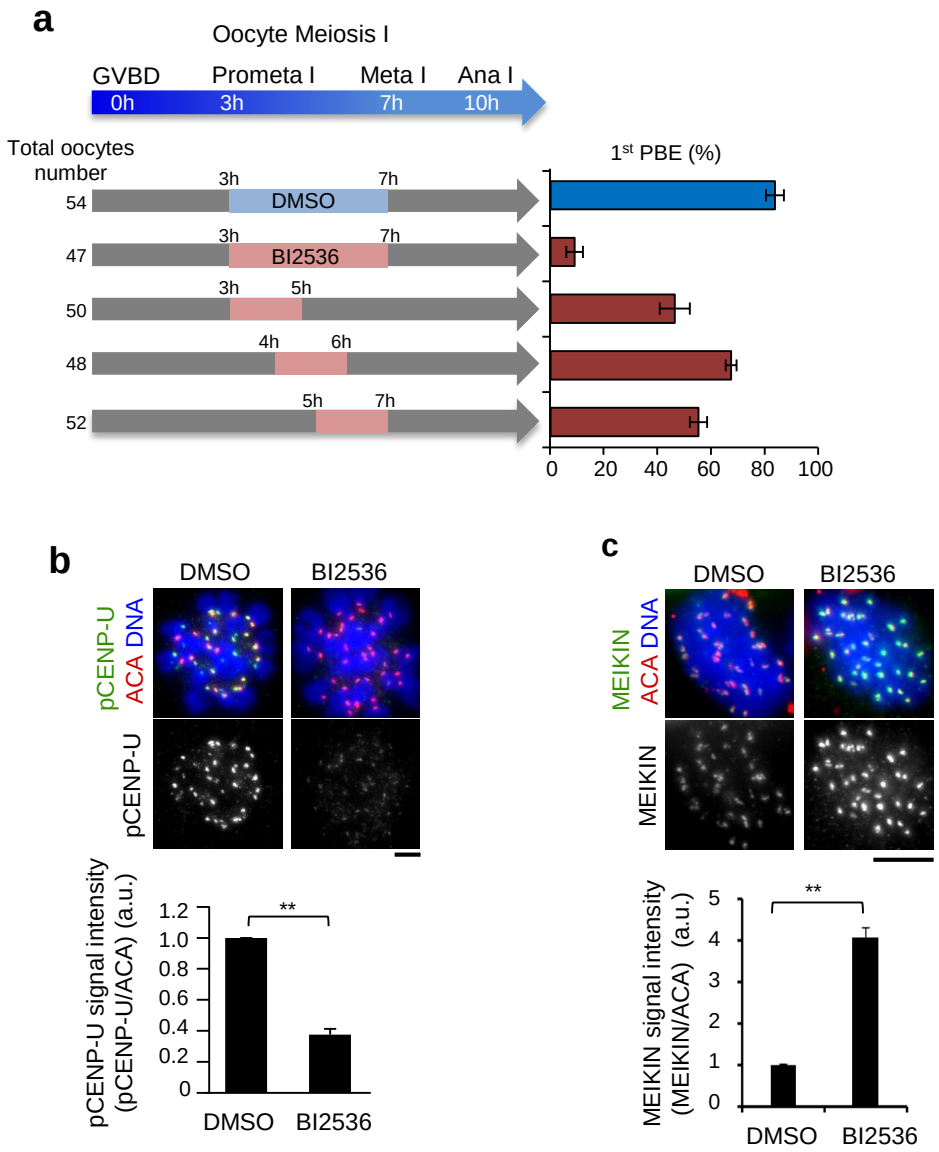

Figure 16. BI2536 treatment reduces PLK1 kinase activity and inhibits MEIKIN degradation
a, Schematic illustration of BI2536 treatment in wild-type oocytes culture (left). Oocytes were treated with DMSO or BI 2536 (100 nM) during the indicated time periods, then washed and released into normal culture medium. 1st polar body extrusion ratio (1st PBE) was counted at 10 h after GVBD (right). Error bars, mean ± s.e.m. from 3 independent experiments. The total number of oocytes used for 3 experiments is shown. **b,** Wild-type oocytes treated with DMSO or BI2536 (during 6-7 h post GVBD) were fixed and immunostained for PLK1 substrate pCENP-U, ACA and DAPI at metaphase I (upper). The relative pCENP-U intensity normalized to that of ACA is shown in the graph with mean + s.e.m. from 3 independent experiments. In each experiment, 10 kinetochores from an oocyte were quantified (n = 4 cells) **c,** Wild-type spermatocytes treated 1 hour with DMSO or BI2536 were fixed and immunostained for MEIKIN, ACA and DAPI at metaphase I (upper). The relative MEIKIN intensity normalized to that of ACA is shown by the graph with mean + s.e.m. from 3 independent experiments. In each experiment, 15 kinetochores from a spermatocyte were quantified (n = 4cells). ***P* < 0.01, unpaired *t*-test (**b-c**). Scale bars, 5 μm.

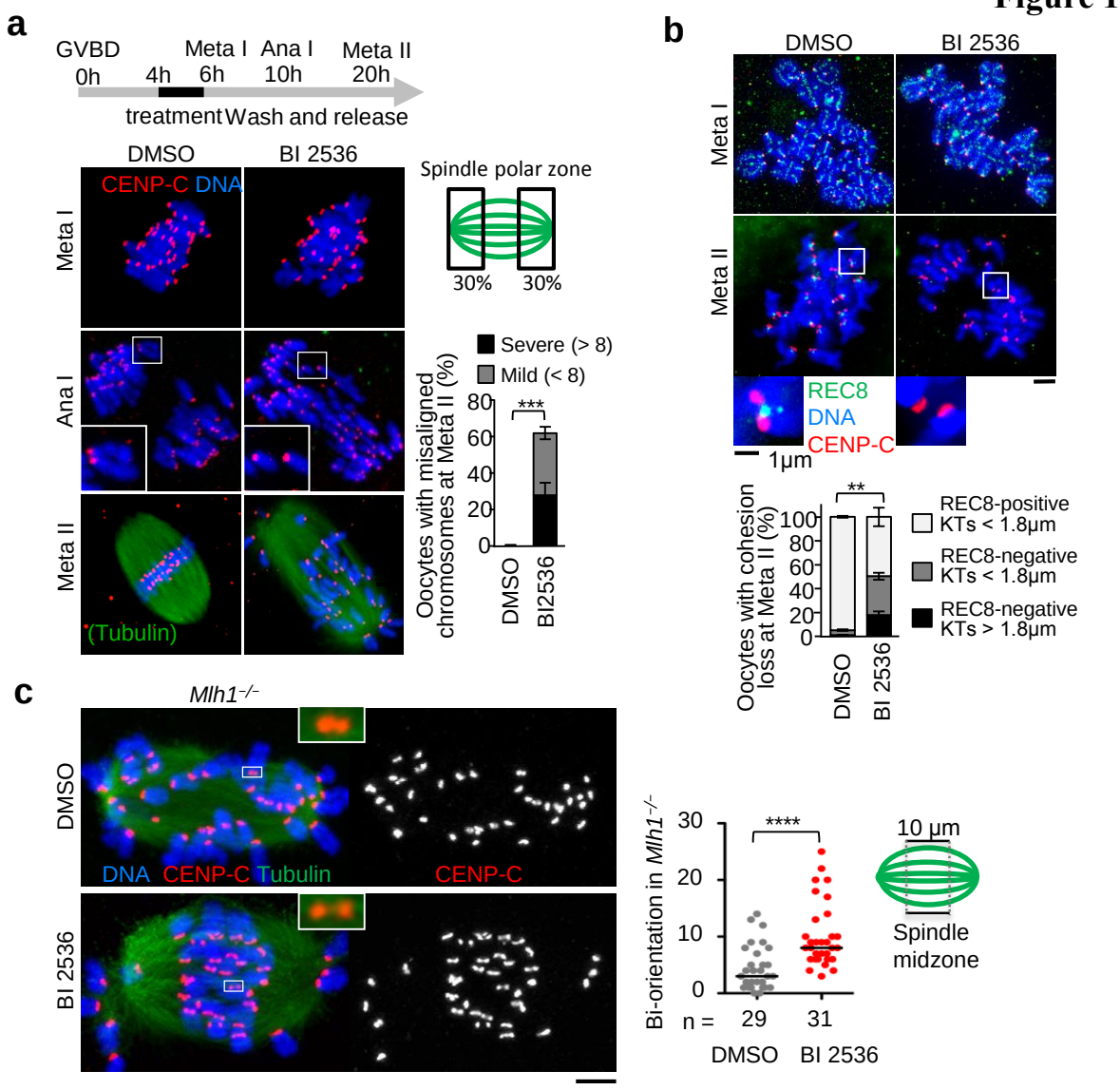

Figure 17. PLK1 is required for protection of centromeric cohesion and mono-orientation.
a, A schematic time course of PLK1 inhibition experiment in wild-type oocytes (upper). Oocytes were treated with DMSO or BI 2536 during 4-6 h post GVBD and stained for α-tubulin, CENP-C and DAPI at the indicated stages in whole mount (bottom left). Magnified images are shown to highlight the separation of sister kinetochores in BI 2536-treated oocyte in anaphase I. The number of single chromatids at the spindle polar zone was scored at metaphase II (bottom right). Error bars, mean ± s.e.m. from 3 independent experiments. 10 oocytes were counted in each experiment. *P*-values indicate the outcome of unpaired *t*-test from misalignment categories. **b,** Chromosome spreads from control and BI 2536-treated wild-type oocytes at metaphase I (6 h post GVBD) and metaphase II (20 h post GVBD) were stained for REC8, CENP-C and DAPI (upper). Magnified images are shown to highlight the loss of cohesion in BI 2536-treated oocytes in metaphase II. The spread chromosomes at metaphase II were classified into three categories according to REC8 signals and kinetochore distance. Each category is shown in the graph with mean ± s.e.m. from 3 independent experiments. 5 oocytes were counted in each experiment (bottom). *P*-values indicate the outcome of unpaired *t*-test from REC8-negative categories. **c,** *Mlh1*$^{-/-}$ oocytes were treated with BI 2536 between 9-10 h post GVBD and then stained for α-tubulin, CENP-C and DAPI in whole mount (left). Magnified images are shown to highlight bi-oriented sister kinetochores at the spindle midzone. Bi-oriented sister kinetochores were scored (right) as indicated in Fig. 13c. $^{**}P < 0.01$, $^{***}P < 0.001$, $^{****}P < 0.0001$, unpaired *t*-test (a-**c**). Scale bars, 5 μm .

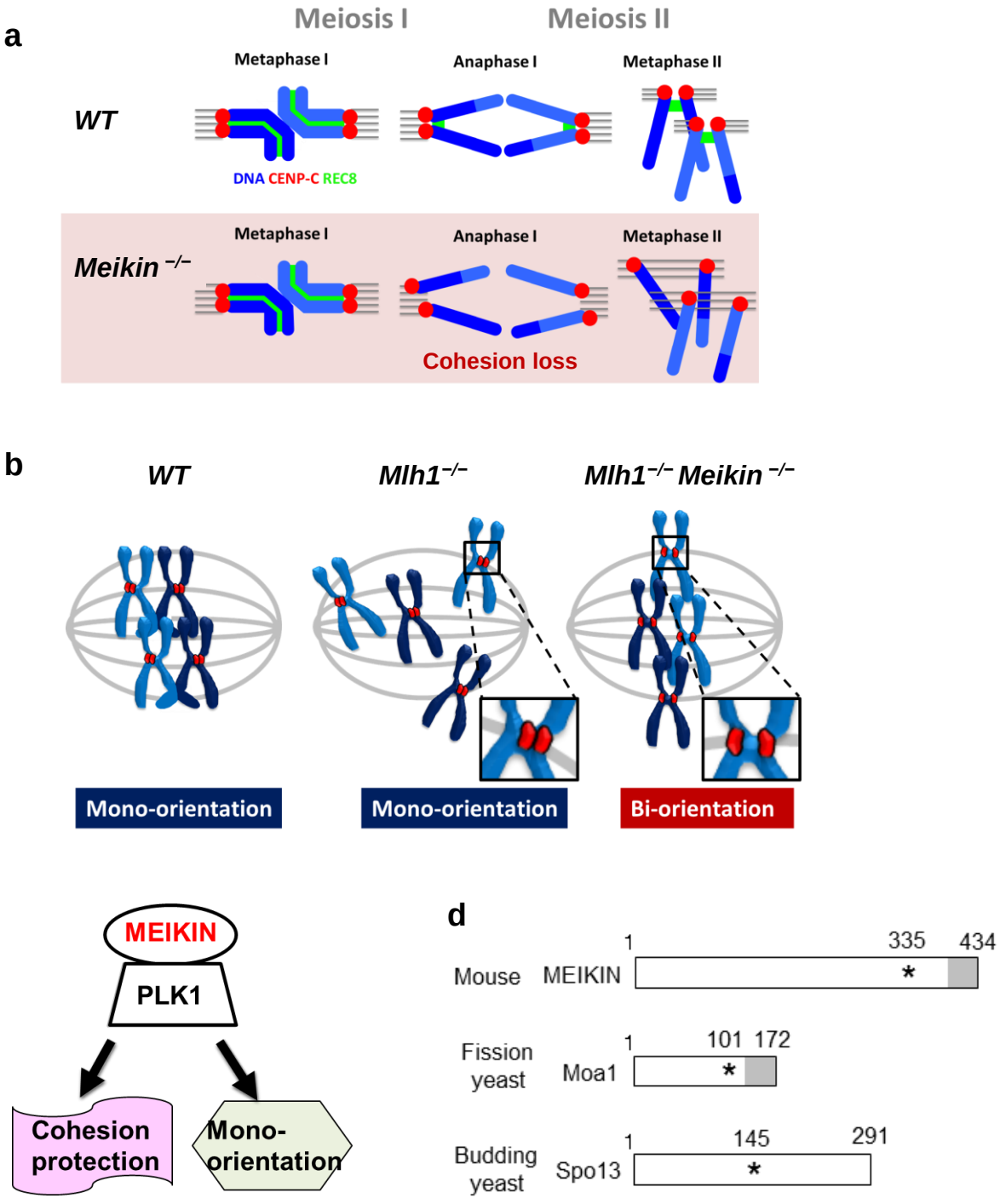

Figure 18. Model of MEIKIN regulation

a, Schematic Model of cohesion protection defects in *Meikin*$^{-/-}$ mice. **b,** Schematic Model of mono-orientation defects of sister kinetochores in *Mlh1*$^{-/-}$ *Meikin*$^{-/-}$ mice. **c,** Schematic Model of meiotic kinetochore regulation by MEIKIN, which cooperates with PLK. **d,** Schematic representation of mouse MEIKIN, fission yeast Moa1 and budding yeast Spo13. Asterisks indicate the polo-box binding motif (STP). Shaded boxes indicate the CENP-C binding region.